

Vorton formation

C. J. A. P. Martins* and E. P. S. Shellard†

*Department of Applied Mathematics and Theoretical Physics, University of Cambridge, Silver Street,
Cambridge CB3 9EW, United Kingdom*

(Received 7 November 1997; published 15 May 1998)

In this paper we present the first analytic model for vorton formation. We start by deriving the microscopic string equations of motion in Witten's superconducting model, and show that in the relevant chiral limit these coincide with the ones obtained from the supersonic elastic models of Carter and Peter. We then numerically study a number of solutions of these equations of motion and thereby suggest criteria for deciding whether a given superconducting loop configuration can form a vorton. Finally, using a recently developed model for the evolution of currents in superconducting strings we conjecture, by comparison with these criteria, that string networks formed at the GUT phase transition should produce no vortons. On the other hand, a network formed at the electroweak scale can produce vortons accounting for up to 6% of the critical density. Some consequences of our results are discussed. [S0556-2821(98)05312-0]

PACS number(s): 98.80.Cq, 11.27.+d

I. INTRODUCTION

As first pointed out by Witten [1], cosmic strings can in some circumstances (typically when the electromagnetic gauge invariance is broken inside the string) behave as "superconducting wires" carrying large currents and charges—up to the order of the string mass scale in appropriate units. The charge carriers can be either bosons or fermions (see [2] for a review). The former type occurs when it becomes energetically favorable for a charged Higgs field to have a non-zero vacuum expectation value in the string core; the latter happens when fermions couple to the string fields, creating fermion zero modes.

It is well known that arbitrarily large currents are not allowed—there is a critical value beyond which the current saturates. In other words, for large enough winding number per unit length, the superconducting condensate is quenched down, suppressing the current flow. Also, the current can decay by magnetic flux-line tunnelling; this can be used to impose constraints on allowed particle physics models.

If superconducting strings carry currents, they must also carry charges of similar magnitude. This includes not only charges trapped at formation by the Kibble mechanism but also the ones due to string inter-commuting between regions of the string network with different currents. Just like with currents, charge densities cannot have arbitrarily large magnitude—there is a limit beyond which there will no longer be an energy barrier preventing the charge carriers from leaving the string.

A rather important point is that the presence of charges on the string tends to counteract the current quenching effect discussed above. In fact, numerical simulations of contracting string loops at fixed charge and winding number have shown [3] that a "chiral" state with equal charge and current densities is approached as the loop contracts. In this limiting chiral case, quenching is in fact eliminated completely. This

has several important consequences. Strings that have trapped charges as a consequence of a phase transition can become superconducting even if the formation of a condensate was otherwise energetically unfavored. More importantly, a string with both a charge and a current density will have a non-zero angular momentum.

In the cosmological context, these strings would of course interact with the cosmic plasma, originating a number of interesting consequences. The most remarkable of these, however, has to do with the evolution of string loops. If a superconducting string loop has an angular momentum, it is semi-classically conserved, and it tries to resist the loop's tension. This will at least increase the loop's lifetime. If the current is too large, charge carriers will leave the string accompanied by a burst of electromagnetic radiation, but otherwise it is possible that dynamically stable loops form. These are called vortons [4]—they are stationary rings that do not radiate classically, and at large distances they look like point particles with quantized charge and angular momentum. Their cosmological significance comes from the fact that they provide very strong constraints on allowed particle physics models, since they behave like non-relativistic particles. According to current belief [4,5], if they are formed at high enough energy scales, they are as dangerous as magnetic monopoles, producing an over-density of matter in disagreement with observations. On the other hand, low-mass vortons could be a very interesting dark matter candidate. Understanding the mechanisms behind formation and evolution is therefore an essential cosmological task.

The overwhelming majority of the work done on cosmic strings so far has been concerned with the structureless Goto-Nambu strings (but see [6] and references therein for some exceptions). In the case of work on vortons, this means that somewhat *ad hoc* estimates had to be made for some properties of the cosmic string network—notably for microscopic quantities such as current and charge densities. This is despite the fact it was recognized a long time ago that, even though they might be computationally very useful [7–9], Goto-Nambu models cannot realistically be expected to account for a number of cosmologically relevant phenomena, due to the very limited number of degrees of freedom avail-

*Also at C. A. U. P., Rua do Campo Alegre 823, 4150 Porto, Portugal. Electronic address: C.J.A.P.Martins@damtp.cam.ac.uk

†Electronic address: E.P.S.Shellard@damtp.cam.ac.uk

able. Two such phenomena are the buildup of small-scale structure and charge and current densities.

In this paper we fill this important gap by discussing the problem of vorton formation in the context of the superconducting string models of Witten [1] and of Carter and Peter [10] (Secs. II and III). Strangely enough, the issue of the conditions for vorton formation has been so far neglected with respect to those of their stability and cosmological consequences. We will start by introducing these models and determining the microscopic string equations of motion in each case. It will be shown that in the relevant chiral limit these equations coincide—this also provides the first conclusive evidence of the validity of the supersonic elastic models of Carter and Peter [10].

We then proceed to study the evolution of a number of loop solutions of these equations numerically (Secs. IV and V), and from the results of this analysis parameters will be introduced which characterize the loop's ability to evolve into a vorton state (Sec. VI). Finally, we discuss a very simple phenomenological model for the evolution of the superconducting currents on the long cosmic string network [11], based on the dynamics of a "superconducting correlation length" (Secs. VII–VIII). Using this model we can therefore estimate the currents carried by string loops formed at all relevant times, and thus (in principle) decide if these can become vortons (Sec. IX) and calculate the corresponding density (Sec. X).

Based on our results, we do not expect any grand unified theory (GUT) vortons to form at all. This is essentially because the friction-dominated epoch is very short for GUT-scale strings [7], and so their currents and charges are never large enough to prevent them from becoming relativistic—and therefore liable to losses. Even if they did form, they would not be in conflict with the standard cosmological scenario if they decayed soon after the end of the friction-domination epoch.

Hence we conclude that, in contrast with previously existing estimates [4,5], one cannot at the moment rule out GUT superconducting string models. We should point out at the outset that there are essentially three improvements in the present work which justify the different end result for GUT-scale strings. First, by analyzing simple (but physically relevant) loop solutions of the microscopic string equations of motion for the Witten model, we can get a much improved idea of how superconducting loops evolve and of how (and under which conditions) they reach a vorton state. Second, by using a simple model for the evolution of the currents on the long strings [11] we can accurately determine the typical currents on each string loop at the epoch of its formation. Finally, the use of the analytic formalism previously introduced by the present authors [7,9] allows us to use a quantitative description throughout the paper, and in particular to determine the loop sizes at formation.

As will become clear below, when taken together these allow a detailed analysis of the process of vorton formation to be carried out, in either the Witten model (as is done in this paper) or any other that one considers relevant. In contrast, note that Davis and Shellard [4] restrict themselves to the particular case of the initial Brownian Vachaspati-Vilenkin loops with Kibble currents, and do not consider the subsequent evolution of the network. On the other hand,

Brandenberger *et al.* [5] make rather optimistic order-of-magnitude estimates about the process of relaxation into a vorton state. As it turns out, for high energy GUT scales, all these loops become relativistic before reaching a vorton state. Finally, neither of these treatments has the benefit of a quantitative model for the evolution of the long-string network [7] which allows one to accurately describe the process of loop production.

On the other hand, as we lower the string-forming energy scale we expect more and more efficient vorton production, and the "old" scenario still holds. Therefore intermediate-scale superconducting strings are still ruled out, since they would lead to a universe becoming matter dominated earlier than observationally allowed. Finally, at low enough energy scales, vortons will be a dark matter candidate. For example, for a string network formed around $T \sim 10^2$ GeV (typical of the electroweak phase transition) they can provide up to 6% of the critical density. A more detailed discussion of these issues is left to a forthcoming publication [12].

Throughout this paper we will use fundamental units in which $\hbar = c = k_B = G m_{Pl}^2 = 1$.

II. WITTEN'S MICROSCOPIC MODEL

As first pointed out by Witten [1], a low-energy effective action for a superconducting string can be derived in a way that is fairly similar to what is done in the Goto-Nambu case (see for example [2]). One has to adopt the additional assumptions that the current is much smaller than the critical current and that the electromagnetic vector potential A_μ is slowly varying on the scale of the condensate thickness.

The derivation then proceeds as in the neutral case, except for the use of the well-known fact that in two dimensions a conserved current can be written as the derivative of a scalar field. One obtains

$$S = \int \sqrt{-\gamma} \left[-\mu_0 + \frac{1}{2} \gamma^{ab} \phi_{,a} \phi_{,b} - q A_\mu x_{,a}^\mu \frac{\epsilon^{ab}}{\sqrt{-\gamma}} \phi_{,b} \right] d^2 \sigma \quad (2.1)$$

$$- \frac{1}{16\pi} \int d^4 x \sqrt{-g} F_{\mu\nu} F^{\mu\nu}; \quad (2.2)$$

the four terms are respectively the usual Goto-Nambu term, the inertia of the charge carriers, the current coupling to the electromagnetic potential and the external electromagnetic field (ϵ^{ab} is the alternating tensor); note that this applies to both the bosonic and the fermionic cases [2].

Recalling the usual definitions

$$A_a = x_{,a}^\mu A_\mu, \quad (2.3)$$

$$F_{ab} = F_{\mu\nu} x_{,a}^\mu x_{,b}^\nu = A_{b,a} - A_{a,b}, \quad (2.4)$$

and defining Y_{ab} to be the stress-energy tensor of the scalar field ϕ ,

$$Y_{ab} = \phi_{,a} \phi_{,b} - \frac{1}{2} \gamma_{ab} \phi_{,c} \phi^{,c}, \quad (2.5)$$

and the conserved current J^a as

$$J^a = q \frac{\epsilon^{ab}}{\sqrt{-\gamma}} \phi_{,b}, \quad (2.6)$$

we can obtain the following equations of motion by varying the action (2.2) with respect to A_μ , ϕ and x^μ respectively:

$$F_{\nu}^{\mu} \equiv -4\pi q j^\mu = -4\pi \int d^2\sigma \epsilon^{ab} x_{,a}^\mu \phi_{,b} \delta^4(x - x(\sigma^a)), \quad (2.7)$$

$$\partial_a(\sqrt{-\gamma} \gamma^{ab} \phi_{,b}) + \frac{1}{2} q \sqrt{-\gamma} \tilde{\epsilon}^{ab} F_{ab} = 0, \quad (2.8)$$

and

$$\begin{aligned} \partial_a \left[\sqrt{-\gamma} \left(\gamma^{ab} + \frac{1}{\mu_0} Y^{ab} \right) x_{,b}^\alpha \right] \\ + \sqrt{-\gamma} \left(\gamma^{ab} + \frac{1}{\mu_0} Y^{ab} \right) \Gamma_{\sigma\rho}^\alpha x_{,a}^\sigma x_{,b}^\rho \end{aligned} \quad (2.9)$$

$$= \sqrt{-\gamma} (F^\alpha + f^\alpha), \quad (2.10)$$

where $\Gamma_{\mu\nu}^\alpha$ is the usual metric connection,

$$\Gamma_{\mu\nu}^\alpha = \frac{1}{2} g^{\alpha\lambda} (g_{\alpha\mu,\nu} + g_{\nu\alpha,\mu} - g_{\mu\nu,\alpha}), \quad (2.11)$$

and F^α is the Lorentz force,

$$F^\alpha = \frac{1}{2\mu_0} F_{\nu}^{\alpha} x_{,a}^\nu J^a. \quad (2.12)$$

We have also included the friction force

$$f^\alpha = \frac{1}{l_f} (u^\alpha - x_{,a}^\alpha x^{\sigma,a} u_\sigma), \quad (2.13)$$

using the same procedure as described in [13,7]. As shown in [11], plasma effects are subdominant, except possibly in the presence of background magnetic fields—either of ‘‘primordial’’ origin or generated (typically by a dynamo mechanism) once proto-galaxies have formed. Hence one expects Aharonov-Bohm scattering [14] to be the dominant effect, and consequently we have [7]

$$l_f = \frac{\mu}{\beta T_b^3}, \quad (2.14)$$

where T_b is the background temperature and β is a numerical factor related to the number of particle species interacting with the string.

The effect of self-inductance leads to the renormalization of both the electromagnetic coupling and the scalar field ϕ . Now, it is well known that the Maxwell-Faraday tensor includes both the external field and the field produced by the string itself, but it can be shown that if one follows this renormalization procedure, one can identify it with its external component, which henceforth we assume to vanish [2].

As we already pointed out, when dealing with superconducting string loops we are essentially interested in the chiral limit of this model, that is

$$\gamma_{ab} J^a J^b = 0, \quad (2.15)$$

or equivalently

$$\phi'^2 = \epsilon^2 \dot{\phi}^2. \quad (2.16)$$

In this limit, introducing the simplifying function Φ defined as

$$\Phi(\chi) = \frac{\dot{\phi}^2}{\mu_0 \gamma_{00}}, \quad (2.17)$$

and choosing the standard gauge conditions

$$\sigma^0 = \tau, \quad \dot{\mathbf{x}} \cdot \mathbf{x}' = 0 \quad (2.18)$$

(with overdots and primes respectively denoting derivatives with respect to the time-like and space-like coordinates on the worldsheet as usual) the string equations of motion in a Friedman-Robertson-Walker (FRW) background with the line element

$$ds^2 = a^2(d\tau^2 - d\mathbf{x}^2) \quad (2.19)$$

[which implies that $\gamma_{00} = a^2(1 - \dot{\mathbf{x}}^2)$] have the form

$$[\epsilon(1 + \Phi)]' + \frac{\epsilon}{l_d} \dot{\mathbf{x}}^2 = \Phi' - 2\frac{\dot{a}}{a} \epsilon \Phi \quad (2.20)$$

and

$$\begin{aligned} \epsilon(1 + \Phi) \ddot{\mathbf{x}} + \frac{\epsilon}{l_d} (1 - \dot{\mathbf{x}}^2) \dot{\mathbf{x}} = & \left[(1 - \Phi) \frac{\mathbf{x}'}{\epsilon} \right]' \\ & + \left(\dot{\Phi} + 2\frac{\dot{a}}{a} \Phi \right) \mathbf{x}' + 2\Phi \dot{\mathbf{x}}', \end{aligned} \quad (2.21)$$

where for simplicity we have introduced the ‘‘damping length’’

$$\frac{1}{l_d} = a \left(2H + \frac{1}{l_f} \right). \quad (2.22)$$

Finally, the worldsheet charge and current densities are respectively given by

$$\rho_w = q \epsilon \dot{\phi} \quad (2.23)$$

and

$$j_w = q \frac{\phi'}{\epsilon}. \quad (2.24)$$

Note that the Witten action is ‘‘microscopic’’ in the sense of being built using only the properties of the underlying particle physics model [1]. In the next section we will ana-

lyze the equations of motion obtained from the action for the elastic supersonic models of Carter and Peter [10], which is in this sense “macroscopic.”

III. SUPERSONIC ELASTIC MODELS

In order to account for phenomena such as the buildup of charge and current densities on cosmic strings, one must introduce additional degrees of freedom on the string worldsheet. One such class of models, originally introduced by Carter and co-workers, is usually referred to as elastic models (see [6] and references therein, on which the following two subsections are based).

A. Basics of elastic models

In general, elastic string models can be described by a Lagrangian density depending on the spacetime metric $g_{\mu\nu}$, background fields such as a Maxwellian-type gauge potential A_μ or a Kalb-Ramond gauge field $B_{\mu\nu}$ (but not their gradients) and any relevant internal fields (which will be discussed in detail below). Note that the Goto-Nambu model has a constant Lagrangian density: namely

$$\mathcal{L}_{GN} = -\mu_0. \quad (3.1)$$

Upon infinitesimal variations in the background fields, and provided that independent internal fields are kept fixed (or alternatively that their dynamic equations of motion are satisfied), the action will change by

$$\delta S = -\frac{1}{2} \int (T^{\mu\nu} \delta g_{\mu\nu} + W^{\mu\nu} \delta B_{\mu\nu} + 2J^\mu A_\mu) \sqrt{-\gamma} d^2\sigma, \quad (3.2)$$

where

$$T^{\mu\nu} = 2 \frac{\delta \mathcal{L}}{\delta g_{\mu\nu}} + \mathcal{L} \eta^{\mu\nu} \quad (3.3)$$

is the worldsheet stress-energy tensor density,

$$J^\mu = \frac{\delta \mathcal{L}}{\delta A_\mu} \quad (3.4)$$

is the worldsheet electromagnetic current density, and

$$W^{\mu\nu} = 2 \frac{\delta \mathcal{L}}{\delta B_{\mu\nu}} \quad (3.5)$$

is the worldsheet vorticity flux. The later will not be considered further in this paper.

It useful to define two orthogonal unit vectors tangent to the worldsheet, one of them being time-like and the other space-like, such that

$$-U^\mu U_\mu = V^\mu V_\mu = 1, \quad U^\mu V_\mu = 0. \quad (3.6)$$

The eigenvalues of this ortho-normal frame are the energy density in the locally preferred string rest frame, which will henceforth be denoted by U , and the local string tension, denoted T [there should be no confusion with the vector U^μ

defined in Eq. (3.6) and the stress-energy tensor $T^{\mu\nu}$ defined in Eq. (3.3), respectively], so that one can write

$$T^{\mu\nu} = U U^\mu U^\nu - T V^\mu V^\nu. \quad (3.7)$$

Note that U and T are simply constants for a Goto-Nambu string,

$$U = T = \mu_0, \quad (3.8)$$

but they are variable in general—hence the name “elastic strings.” In particular, one should expect that the string tension in an elastic model will be reduced with respect to the Goto-Nambu case due to the mechanical effect of the current.

Since elastic string models necessarily possess conserved currents, it is convenient to define a “stream function” ψ on the worldsheet that will be constant along the current’s flow lines. The part of the Lagrangian density \mathcal{L} containing the internal fields is usually called the “master function,” and can be defined as a function of the magnitude of the gradient of this stream function, $\Lambda = \Lambda(\chi)$, such that

$$\chi = \gamma^{ab} \psi_{;a} \psi_{;b}, \quad (3.9)$$

where the gauge covariant derivative is defined as

$$\psi_{;a} = \partial_a \psi - e A_{\mu a} x^\mu. \quad (3.10)$$

Note that the definition of χ differs by a minus sign from that of Carter [6]; the reason for this will become clear below. This “dynamic” term contains charge couplings, whose relevance will be further discussed below. Nevertheless, whether or not these or other background gauge fields are present, it is always the form of the master function which determines the equation—or equations—of state.

There is also a dual [15] potential $\tilde{\psi}$, whose gradient is orthogonal to that of ψ , and the corresponding dual master function $\tilde{\Lambda} = \tilde{\Lambda}(\tilde{\chi})$ such that

$$\tilde{\chi} = \gamma^{ab} \tilde{\psi}_{;a} \tilde{\psi}_{;b}, \quad (3.11)$$

with the obvious definition for $\tilde{\psi}_{;a}$. The duality between these descriptions means that the field equations for the stream function ψ obtained with the master function Λ are the same as those for the dual potential $\tilde{\psi}$ obtained with the dual master function $\tilde{\Lambda}$. However, there will in general be two different equation of state relating the energy density U and the tension T ; these correspond to what is known as the “magnetic” and “electric” regimes, respectively corresponding to the cases

$$\tilde{\chi}_{mg} < 0 < \chi_{mg} \quad (3.12)$$

and

$$\chi_{el} < 0 < \tilde{\chi}_{el}, \quad (3.13)$$

which are respectively characterized by space-like and time-like currents. In the degenerate null state limit, however, there will be a single equation

$$U = T = \mu_0. \quad (3.14)$$

Note that the distinction between a given model and its dual disappears in the absence of charge couplings; such models are then called ‘‘self-dual’’ for obvious reasons.

In each case the equation of state provides the expressions

$$c_E^2 = \frac{T}{U}, \quad (3.15)$$

$$c_L^2 = -\frac{dT}{dU} = \frac{\nu}{\mu} \frac{d\mu}{d\nu}, \quad (3.16)$$

for the extrinsic (that is transverse, or ‘‘wobble’’) and for the sound-type (longitudinal or ‘‘wobble’’) perturbations of the worldsheet. Both of these must obey $c^2 \geq 0$ (a requirement for local stability) and $c^2 \leq 1$ (a requirement for local causality). These two speeds can be used to characterize the elastic model in question; in particular there is a straightforward but quite meaningful division of the models into supersonic (that is, those obeying $c_E > c_L$), transonic ($c_E = c_L$; only in the null limit is this common speed unity) and subsonic ($c_E < c_L$).

B. Supersonic (superconducting) models

Carter and Peter [10] have recently proposed two supersonic elastic models to describe the behavior of current-carrying cosmic strings. The Lagrangian density in the magnetic regime is

$$\tilde{\Lambda}_{mg} = -m^2 + \frac{\tilde{\chi}}{2} \left(1 - \frac{\tilde{\chi}}{2k_0 m_\sigma^2} \right)^{-1}, \quad (3.17)$$

m_σ being the current carrier mass (which is at most of the order of the relevant Higgs mass); this is valid in the range

$$-\frac{1}{3} < \frac{\tilde{\chi}}{k_0 m_\sigma^2} < 1 - \frac{k_0 m_\sigma^2}{2m^2 + k_0 m_\sigma^2}, \quad (3.18)$$

and obeys the equation of state

$$\frac{U}{m^2} = 1 + \frac{k_0 m_\sigma^2}{4m^2} - \frac{\sqrt{k_0}}{\sqrt{2}} \frac{m_\sigma}{m} \left(\frac{T}{m^2} - 1 + \frac{k_0 m_\sigma^2}{8m^2} \right)^{1/2}. \quad (3.19)$$

On the other hand, the electric regime is described by the Lagrangian density

$$\tilde{\Lambda}_{el} = -m^2 - \frac{k_0 m_\sigma^2}{2} \ln \left(1 - \frac{\tilde{\chi}}{k_0 m_\sigma^2} \right), \quad (3.20)$$

which is valid in the range

$$-1 < \frac{\tilde{\chi}}{k_0 m_\sigma^2} < 1 - e^{-2m^2/k_0 m_\sigma^2}, \quad (3.21)$$

and the corresponding equation of state is

$$\frac{U}{m^2} = \frac{T}{m^2} + \frac{k_0 m_\sigma^2}{m^2} \left[\exp \left(2 \frac{1 - T/m^2}{k_0 m_\sigma^2/m^2} \right) - 1 \right]. \quad (3.22)$$

These models are supersonic for all space-like and weak time-like currents, with the exception that in the null limit $\tilde{\chi} = 0$ one has $c_L = c_E = 1$.

C. Equations of motion

We now derive the microscopic equations of motion for elastic cosmic string models. It is convenient to start by defining the quantity

$$\Theta^{ab} \equiv \tilde{\Lambda} \gamma^{ab} - 2 \frac{\partial \tilde{\Lambda}}{\partial \tilde{\chi}} \tilde{\psi}^{;a} \tilde{\psi}^{;b}; \quad (3.23)$$

then recalling the definition of $\tilde{\chi}$, Eq. (3.11), one can find the free string equations of motion in the usual (variational) way, obtaining

$$(\sqrt{-\gamma} \Theta^{ab} x_{,b}^\alpha)_{,a} + \sqrt{-\gamma} \Theta^{ab} \Gamma_{\mu\nu}^\alpha x_{,a}^\mu x_{,b}^\nu = 0. \quad (3.24)$$

Also in a similar way to what was done in Sec. II, the effect of the frictional forces is accounted for by introducing a term $\sqrt{-\gamma} F^\alpha$ on the right-hand side of Eq. (3.24). For exactly the same reasons as those of Sec. II, we will have

$$F^\alpha = -\beta T_b^3 (u^\alpha - x_{,a}^\alpha x^{\beta,a} u_\beta). \quad (3.25)$$

However, it should be remarked that the generalized definition of the friction length scale for elastic models is

$$l_f = -\frac{\tilde{\Lambda}}{\beta T_b^3} \quad (3.26)$$

(note that $\tilde{\Lambda}$ is negative).

Of course we now have a further equation for the scalar field $\tilde{\psi}$, namely

$$\partial_a \left(\sqrt{-\gamma} \frac{\partial \tilde{\Lambda}}{\partial \tilde{\chi}} \gamma^{ab} \tilde{\psi}_{;b} \right) = 0. \quad (3.27)$$

Furthermore, the spacetime energy-momentum tensor and electromagnetic current will be given by

$$\sqrt{-g} T^{\mu\nu} = - \int \sqrt{-\gamma} \Theta^{ab} x_{,a}^\mu x_{,b}^\nu \delta(x - x(\sigma, \tau)) d^2 \sigma \quad (3.28)$$

and

$$\sqrt{-g} J^\mu = -2e \int \sqrt{-\gamma} \gamma^{ab} \frac{\partial \tilde{\Lambda}}{\partial \tilde{\chi}} \tilde{\psi}_{;a} x_{,b}^\mu \delta(x - x(\sigma, \tau)) d^2 \sigma. \quad (3.29)$$

The total string energy and charge in a spacetime where the line element is Eq. (2.19) are then defined as [we are again using the gauge choice (2.18)]

$$E = \int \mathbf{d}^3 \mathbf{x} \sqrt{-g} T_0^0 = a \int \left(-\tilde{\Lambda} + 2 \frac{\partial \tilde{\Lambda}}{\partial \tilde{\chi}} \tilde{\psi}_{;0} \tilde{\psi}^{;0} \right) \epsilon d\sigma \quad (3.30)$$

and

$$Q = \int \mathbf{d}^3\mathbf{x} \sqrt{-^{(3)}g} J_0 = -2ea \int \frac{\partial \tilde{\Lambda}}{\partial \tilde{\chi}} \tilde{\psi}_{;0} \epsilon d\sigma. \quad (3.31)$$

The corresponding worldsheet charge and current densities are defined via

$$j^\mu = -2e \frac{\partial \tilde{\Lambda}}{\partial \tilde{\chi}} \sqrt{-\gamma} \gamma^{ab} \tilde{\psi}_{;a} x^\mu_{;b} \equiv x^\mu_{;b} j^b, \quad (3.32)$$

and have the following values:

$$\rho \equiv j^0 = -2e \frac{\partial \tilde{\Lambda}}{\partial \tilde{\chi}} \epsilon \tilde{\psi}_{;0}, \quad (3.33)$$

$$j \equiv -j^1 = -2e \frac{\partial \tilde{\Lambda}}{\partial \tilde{\chi}} \frac{\tilde{\psi}_{;1}}{\epsilon}. \quad (3.34)$$

Again, for the reasons explained above, a particularly relevant situation will be that of a chiral current, that is one in which

$$\gamma_{ab} j^a j^b = 0. \quad (3.35)$$

This is equivalent to

$$\tilde{\psi}'^2 = \epsilon^2 \tilde{\psi}^2, \quad (3.36)$$

and therefore it implies that

$$\frac{\partial \rho}{\partial \tau} = \frac{\partial j}{\partial \sigma} \quad (3.37)$$

and that the total (spacetime) charge and current are also equal. Note that in the chiral case one also has

$$\tilde{\chi} = 0, \quad 2 \frac{\partial \tilde{\Lambda}}{\partial \tilde{\chi}} = 1, \quad (3.38)$$

and so this is not equivalent to the Goto-Nambu case despite the fact that the equation of state is

$$U = T = \mu_0. \quad (3.39)$$

Last but not least, one can always define the fundamental worldsheet current density vector

$$i^a = -\sqrt{-\gamma} \frac{\partial \tilde{\Lambda}}{\partial \tilde{\psi}_{;a}} = 2 \sqrt{-\gamma} \frac{\partial \tilde{\Lambda}}{\partial \tilde{\chi}} \gamma^{ab} \tilde{\psi}_{;b}. \quad (3.40)$$

Although we have included the charge coupling term in the master function and its dual, it should be said that charge coupling effects are subdominant, and thus for most purposes they can be neglected (if nothing else, at least to a first-order approximation). This has been confirmed by Peter [16], and is a consequence of the smallness of the coupling constants—for example, the electromagnetic coupling constant is $e^2 \sim 1/137$. In most of what follows we will therefore neglect the charge coupling.

If an electromagnetic coupling does exist, it will be simply given by

$$i^\mu = e j^\mu, \quad (3.41)$$

where

$$i^\mu = x^\mu_{;a} i^a \quad (3.42)$$

is the corresponding spacetime current. Note that Eq. (3.27) is then just a Noether identity,

$$i^a_{;a} = 0. \quad (3.43)$$

D. Chiral limit

We now consider the (common) chiral limit of the two supersonic elastic models of Carter and Peter [10], defined by the Lagrangian densities (3.17) and (3.20), respectively, for the magnetic and electric regimes. Also, as we did in Sec. II for the Witten model, we will interpret the charge coupling and the scalar field as being renormalized and neglect the coupling to external electromagnetic fields.

Then, with our usual gauge choices and definitions of the damping and friction length scales, the microscopic string equations of motion (3.24) simplify to

$$[\epsilon(1 + \Psi)]' + \frac{\epsilon}{l_d} \dot{\mathbf{x}}^2 = \Psi' - 2 \frac{\dot{a}}{a} \epsilon \Psi \quad (3.44)$$

and

$$\begin{aligned} \epsilon(1 + \Psi) \ddot{\mathbf{x}} + \frac{\epsilon}{l_d} (1 - \dot{\mathbf{x}}^2) \dot{\mathbf{x}} = & \left[(1 - \Psi) \frac{\mathbf{x}'}{\epsilon} \right]' \\ & + \left(\dot{\Psi} + 2 \frac{\dot{a}}{a} \Psi \right) \mathbf{x}' + 2 \Psi \dot{\mathbf{x}}, \end{aligned} \quad (3.45)$$

where Ψ is defined as

$$\Psi(\tilde{\psi}) = \frac{\tilde{\psi}^2}{\mu_0 \gamma_{00}}. \quad (3.46)$$

That is, these are exactly the same equations of motion as those of Witten's model, Eqs. (2.20),(2.21), if one identifies the corresponding scalar fields:

$$\phi \equiv \tilde{\psi}. \quad (3.47)$$

Then, the worldsheet charge and current densities also coincide:

$$\rho_w = q \epsilon \tilde{\psi}, \quad (3.48)$$

$$j_w = q \frac{\tilde{\psi}'}{\epsilon}. \quad (3.49)$$

Finally, the total energy of a piece of string is given by

$$E = \mu_0 a \int (1 + \Psi) \epsilon d\sigma, \quad (3.50)$$

which we can immediately interpret as being split in an obvious way into a ‘‘string’’ component and a ‘‘current’’ component. This interpretation will be relevant below.

Note that if we had preserved Carter’s original sign conventions, we would have found a difference of a factor of i between the two fields. But the important point is that the equality between the two theories in the chiral limit is not entirely trivial since, as we already pointed out, the motivations behind the build up of each of them are quite different. We have thus provided the first substantive evidence of the validity of the supersonic elastic models of Carter and Peter [10].

IV. CHIRAL LOOPS IN FLAT SPACETIME

We will now study the evolution of current-carrying cosmic string loops, starting by considering the simplest case of circular loops in flat spacetime. We therefore choose the *Ansatz*

$$\mathbf{x}(\tau) = r(\tau)(\sin\theta, \cos\theta, 0); \quad (4.1)$$

we also need an *Ansatz* for the scalar field $\tilde{\psi}$ (or ϕ), which we will take to be

$$\tilde{\psi} = \sqrt{\mu_0}[\mathcal{F}(\tau) + n\sigma]t_c, \quad (4.2)$$

where the winding number per unit σ , n , is a constant (due to the symmetry of our loop solution) and t_c is a characteristic time scale—say the epoch of network formation. The chirality condition implies that

$$\epsilon\dot{\mathcal{F}} = n. \quad (4.3)$$

Then the string equations of motion reduce to

$$\epsilon \left(1 + \frac{n^2 t_c^2}{r^2} \right) = 1, \quad (4.4)$$

$$\ddot{r} + \left(1 - \frac{n^4 t_c^4}{r^4} \right) r = 0, \quad (4.5)$$

together with the constraint

$$|n| \leq \frac{1}{2}. \quad (4.6)$$

Note that opposite signs of n correspond to left and right moving currents; naturally it always appears as n^2 in any relevant equation, and we will therefore be taking n to be positive.

In Fig. 1 we have plotted some relevant evolutionary properties of chiral superconducting loops with different n ’s in flat spacetime. Note that these loops never collapse to zero size, and that their microscopic velocity is always less than unity (unlike in the Goto-Nambu case). Furthermore, there is a static solution with

$$n = \frac{1}{2} = \frac{r}{t_c}, \quad \dot{r} = 0; \quad (4.7)$$

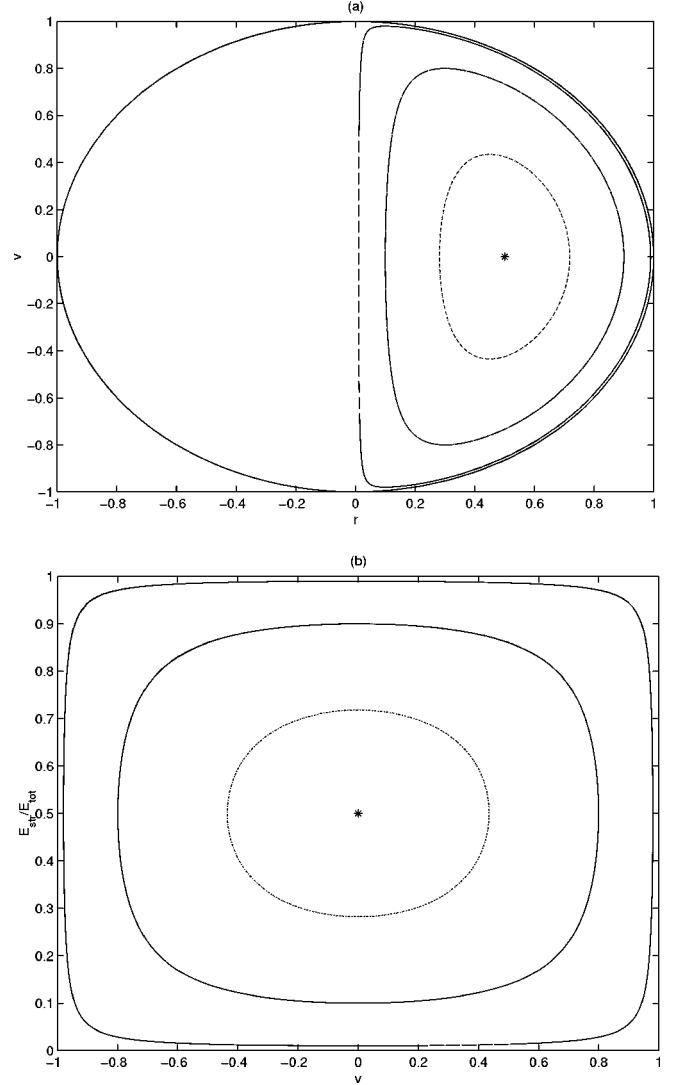


FIG. 1. The flat spacetime evolution of chiral circular string loops characterized by a conserved quantity n [defined in Eq. (4.2)] having the value 0 (solid lines), 0.1 (dashed lines), 0.3 (dot-dashed lines), 0.45 (dotted lines) and 0.5 (star). Note that the first corresponds to a simple Goto-Nambu loop, while the last is a static solution. Plots respectively show \dot{r} as function of r [defined in Eq. (4.1)] (a) and the fraction of the energy in the string as a function of r (b).

in this case the energy is equally divided between the string and the current.

It should also be noted that energy is transferred back and forth between the string and the current as the loop oscillates. We can easily determine the following quantities (the averages are over one oscillation period):

$$\left\langle \frac{r^2}{t_c^2} \right\rangle = \frac{1}{2} - n^2, \quad (4.8)$$

$$\left\langle \frac{t_c^2}{r^2} \right\rangle = \frac{1}{n^2}, \quad (4.9)$$

$$\langle \dot{r}^2 \rangle = \frac{1}{2}(1 - 4n^2), \quad (4.10)$$

while the energy in the string obeys

$$\left\langle \frac{E_{string}}{E_{total}} \right\rangle = 1 - n, \quad (4.11)$$

$$\left\langle \frac{E_{string}^2}{E_{total}^2} \right\rangle = 1 - \frac{3}{2}n; \quad (4.12)$$

note that the energy of these loops is $E_{total}/t_c = 2\pi\mu$.

Finally, we discuss two other points that will have further relevance below. First, a loop with a given conserved number n will reach a maximum microscopic velocity (and corresponding Lorentz factor) given by

$$\dot{r}_{max}^2 = 1 - 4\bar{n}^2, \quad \gamma_{max} = \frac{1}{2\bar{n}}. \quad (4.13)$$

Second, for fixed n and initial velocity, there will be two possible choices of r_i that can be made—the difference is that in one of them most of the energy will be in the string, while in the other it will be in the current. We will call these two cases the “string branch” and the “current branch.” In flat spacetime, the two choices give physically the same solution (they simply correspond to different initial phases of the oscillation), but this will not be true in general.

V. CHIRAL LOOPS IN THE EXPANDING UNIVERSE

The case of circular loops in expanding universes is analogous, and we keep the *Ansätze* for \mathbf{x} and $\tilde{\psi}$:

$$\tilde{\psi} = \sqrt{\mu_0}[\mathcal{F}(\tau) + n\sigma]t_c. \quad (5.1)$$

The winding number per unit σ and the function \mathcal{F} are also constrained as before. In terms of these quantities the total energy of the loop can be written as

$$\begin{aligned} E_{total} &= \mu_0 l_{total} = \mu_0 a \int \left(1 + \frac{n^2 t_c^2}{a^2 r^2} \right) \epsilon d\sigma \\ &\equiv \mu_0 l_{string} + E_{current}, \end{aligned} \quad (5.2)$$

and the loops evolve according to

$$\left(1 + \frac{n^2 t_c^2}{a^2 r^2} \right) \ddot{r} + (1 - \dot{r}^2) \left[\frac{\dot{r}}{l_d} + \left(1 - \frac{n^2 t_c^2}{a^2 r^2} \right) \frac{1}{r} \right] = 0. \quad (5.3)$$

It is convenient to define a macroscopic dimensionless parameter which, as we will show later, turns out to measure the loop’s stability against collapse. We will define it by

$$\bar{n} = \frac{4\pi n t_c}{l_{total}}; \quad (5.4)$$

note that unlike n , which is a constant for each loop, \bar{n} is a variable parameter obeying

$$0 \leq \bar{n} \leq 1; \quad (5.5)$$

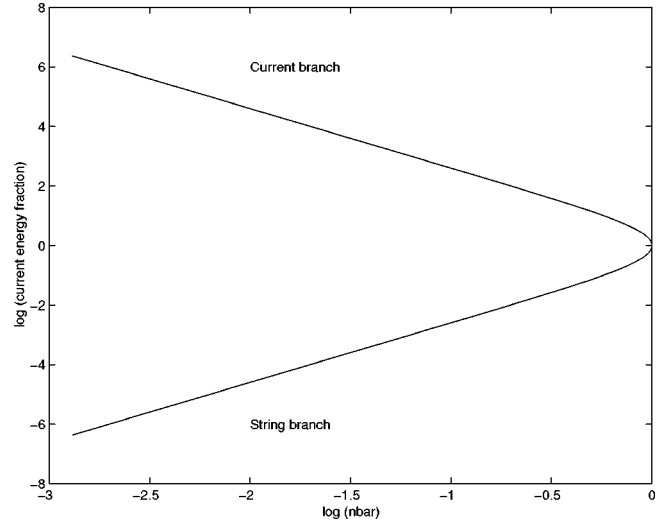


FIG. 2. The logarithm of the ratio of the energies in the current and in the string for chiral circular loops with zero velocity, as a function of the logarithm of parameter \bar{n} . Note that there are two different branches, hereafter called the “current branch” (top) and the “string branch” (bottom).

also $\bar{n} = 0$ corresponds to the Goto-Nambu case, while the $\bar{n} = 1$ limit is the analogous of the flat spacetime static solution, here characterized by

$$E_{string} = E_{current}, \quad \dot{r} = 0; \quad (5.6)$$

in the approach to this limit one can easily establish that the loop’s velocity (in the radiation epoch) and length in string evolve according to

$$v \frac{t}{t_c} = \frac{n}{2}, \quad \frac{l_{string}}{2\pi t_c} = \frac{n}{\sqrt{1 - \dot{r}^2}}; \quad (5.7)$$

these will be numerically confirmed below.

An important difference with respect to the flat spacetime case is that now the string branch and the current branch (see Fig. 2 for a relevant particular case) represent two physically different solutions—something to be expected since damping forces (that is, friction and expansion) act differently on the string and current energies. Since we will be mostly interested in chiral superconducting string loops formed in the friction-dominated regime (as no vortons will form in the “free” regime), we can safely assume that these loops are formed with zero velocity. Now, there is a very simple relation between l_{total} , l_{string} and \bar{n} : namely

$$\frac{l_{total}}{l_{string}} = \frac{2}{\bar{n}^2} (1 \pm \sqrt{1 - \bar{n}^2}). \quad (5.8)$$

The negative sign corresponds to the string branch, where as \bar{n} goes from zero to unity we go from the Goto-Nambu case to the static case where the energy is split equally between the string and the current; the positive sign corresponds to the current branch, where the ratio of the energies in the

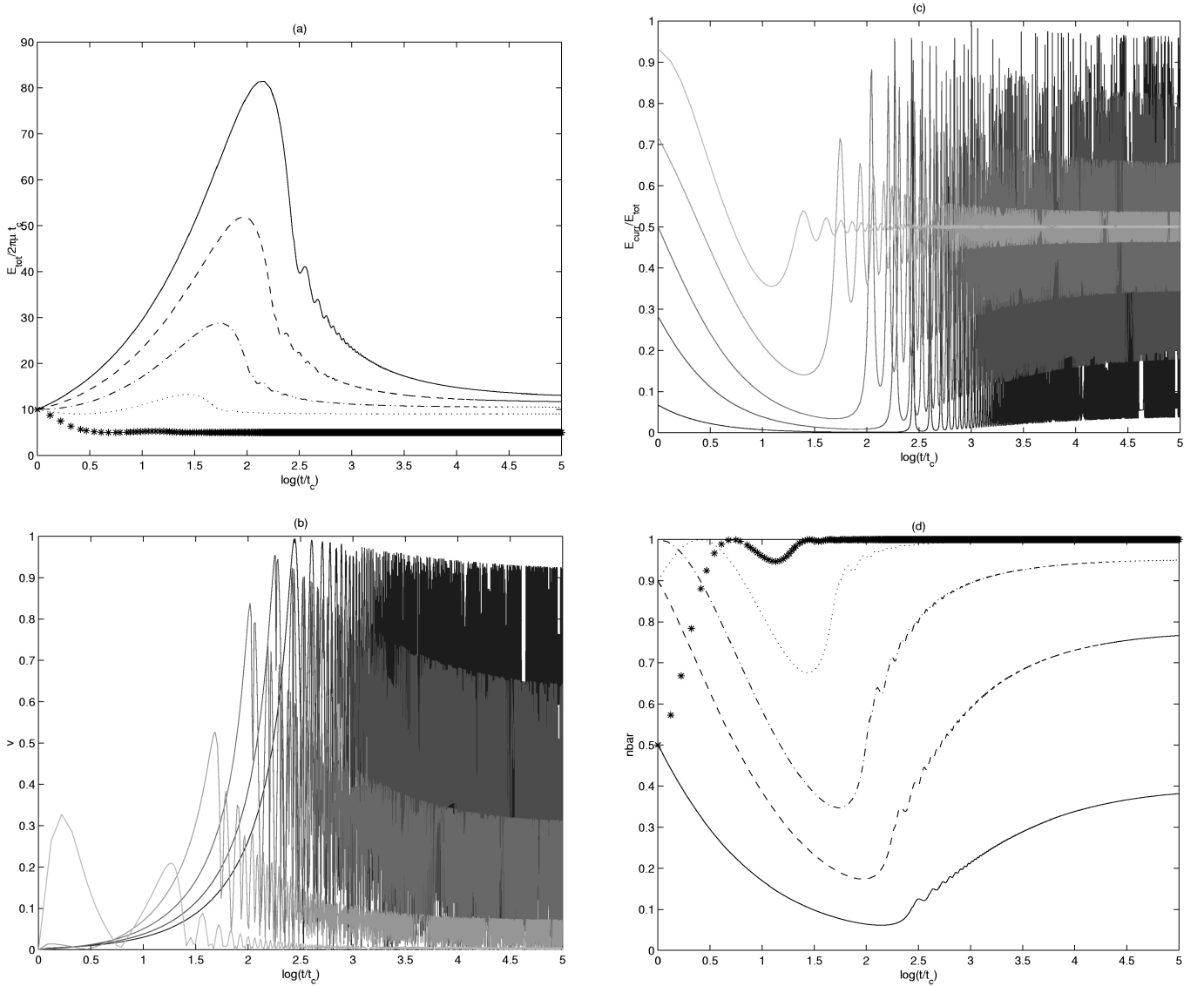


FIG. 3. The evolution of chiral circular GUT-scale string loops formed at $t=t_c$. All loops have an initial total energy $E_{tot}/2\pi\mu t_c = 10$, but different initial string energies—respectively 9.3, 7.2, 5.0, 2.8 and 0.7; in (a) and (d), these are respectively shown in solid, dashed, dash-dotted, dotted and starred lines, while in (b) and (c) they are correspondingly shown by lighter shades of gray. Plots show the total energy E_{total} relative to t_c (a), the microscopic velocity (b), the fraction of the loop’s energy in the current (c) and the parameter \bar{n} defined in Eq. (5.4)(d).

string and in the current decreases until it vanishes when \bar{n} reaches zero again. Note that Eq. (5.8) can be inverted to give

$$\bar{n} = 2 \frac{l_{string}}{l_{total}} \left(\frac{l_{total}}{l_{string}} - 1 \right)^{1/2}. \quad (5.9)$$

In practice, it is not easily conceivable that in cosmological contexts loops can be formed with more energy in the current than in the string itself. Therefore, although for the sake of completeness we will be discussing the current branch in the remainder of this section, we will neglect it afterwards.

Thus from Eq. (5.3) one obtains the evolution equation for $l(l_i, t_i, \bar{n}_i, t)$, $v(l_i, t_i, \bar{n}_i, t)$ and other relevant quantities. As we will see below, a crucial quantity will be the maxi-

mum velocity reached by each loop configuration during its evolution, $v_{max}(l_i, t_i, \bar{n}_i)$. If the loop does become a vorton, then its length will asymptotically be given by $l_v(l_i, \bar{n}_i)$.

In Figs. 3–5 we plot the cosmological evolution of some relevant GUT-scale chiral circular loops. We should mention that in order to save space, only 1 out of every 40 points resulting from the numerical integrations is plotted, and this is the reason why some plots show irregularities.

Figure 3 shows some relevant properties of the evolution of chiral circular GUT-scale loops formed at $t=t_c$; all have an initial total energy $E_{total}/2\pi\mu t_c = 10$, but the distribution of the energy between the string and the current varies.

Obviously, loops with higher currents will have smaller physical radii, and hence they will be less stretched by expansion and enter the horizon earlier, at which point they start oscillating—as can be confirmed in Figs. 3(a),3(b). Re-

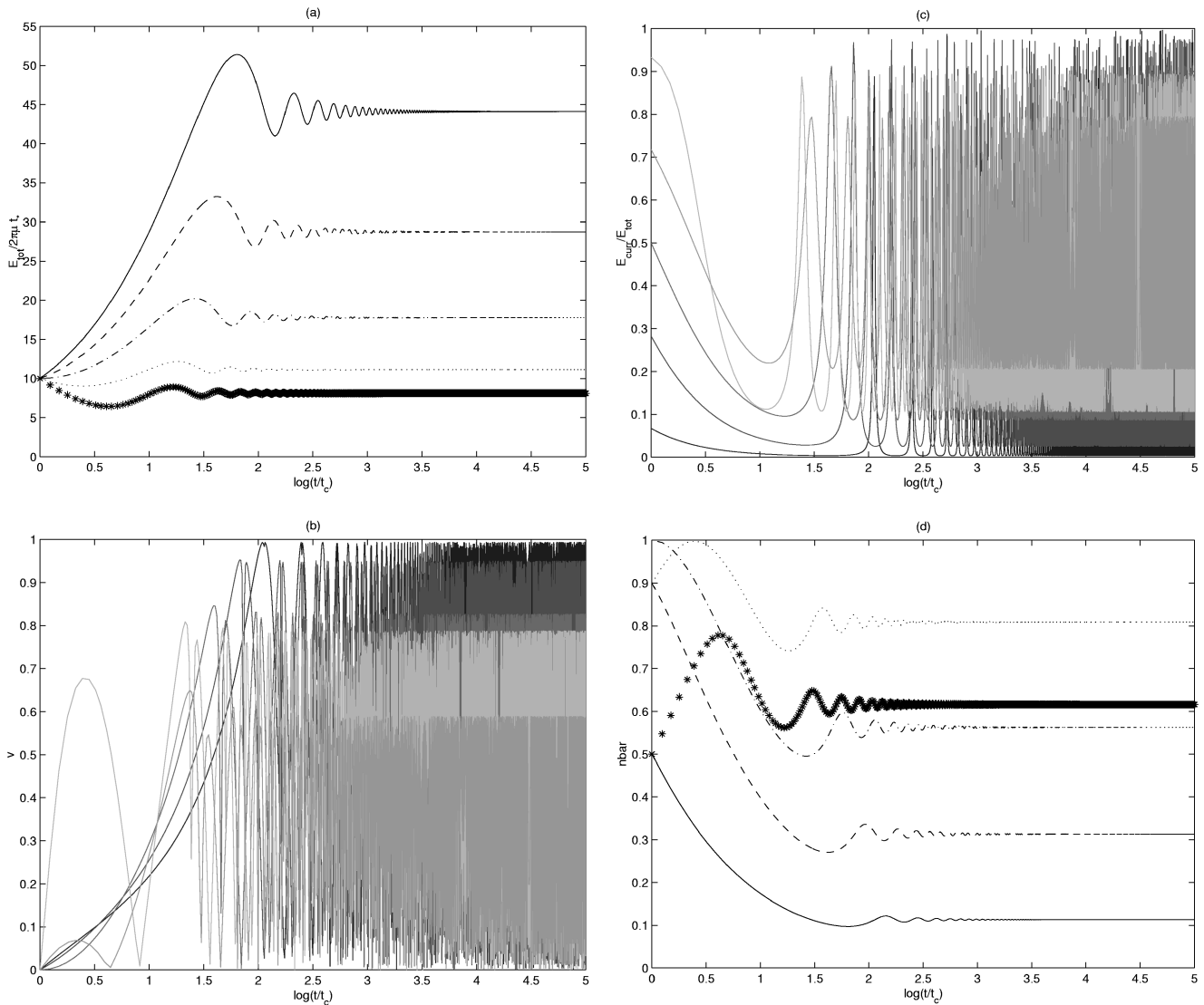


FIG. 4. The evolution of chiral circular GUT-scale string loops formed at $t = t_*$. All loops have an initial total energy $E_{total}/2\pi\mu_* t = 10$, but different initial string energies—respectively 9.3, 7.2, 5.0, 2.8 and 0.7; in (a) and (d), these are respectively shown in solid, dashed, dash-dotted, dotted and starred lines, while in (b) and (c) they are correspondingly shown by lighter shades of gray. Plots show the total energy E_{total} relative to t_* (a), the microscopic velocity (b), the fraction of the loop’s energy in the current (c) and the parameter \bar{n} defined in Eq. (5.4)(d).

garding the velocities, note the significant differences between loops in the “string branch” (which still reach fairly high microscopic velocities, but never $v = 1$) and in the “current branch” (which quickly become non-relativistic). Therefore the latter ones should definitely become vortons, and so it is perhaps fortunate that, as we pointed out above, we do not expect loops with such high currents to be produced in the early universe (at least, for GUT-scale networks). Note that in one of the cases shown the initial current is so high that the loop “overshoots” and acquires a fairly large velocity, but friction quickly slows it down again.

On the other hand, in the string branch the velocity is reduced with respect to the Goto-Nambu case, and a more detailed investigation will be needed to set up some criterion defining which velocities will allow vorton formation—recall that relativistic velocities will imply charge losses and it will therefore be unrealistic to make any definite claims or predictions about such cases.

The evolution of the fraction of the loop’s energy in the current is particularly illuminating [see Fig. 3(c)]. This will obviously decrease while the loop is being stretched, and it will start oscillating when the loop falls in side the horizon. The oscillations are around the state with equipartition of the energy between the string and the current, which as we saw corresponds to a static solution in flat spacetime. Note that the effect of the friction force is to reduce the amplitude of these oscillations, and so one can see that friction is in fact crucial for vorton formation. Naturally, loops with smaller velocities will undergo oscillations with smaller amplitudes, and so again we confirm that these are the strongest vorton candidates. Finally, we have plotted the parameter \bar{n} [which was defined in Eq. (5.4)] in Fig. 3(d), and as one can easily see by comparison with the other three plots this is indeed a good indicator of whether or not a given loop can become a vorton—in fact, the “phenomenological” criterion that we mentioned above will be basically expressed in terms of the

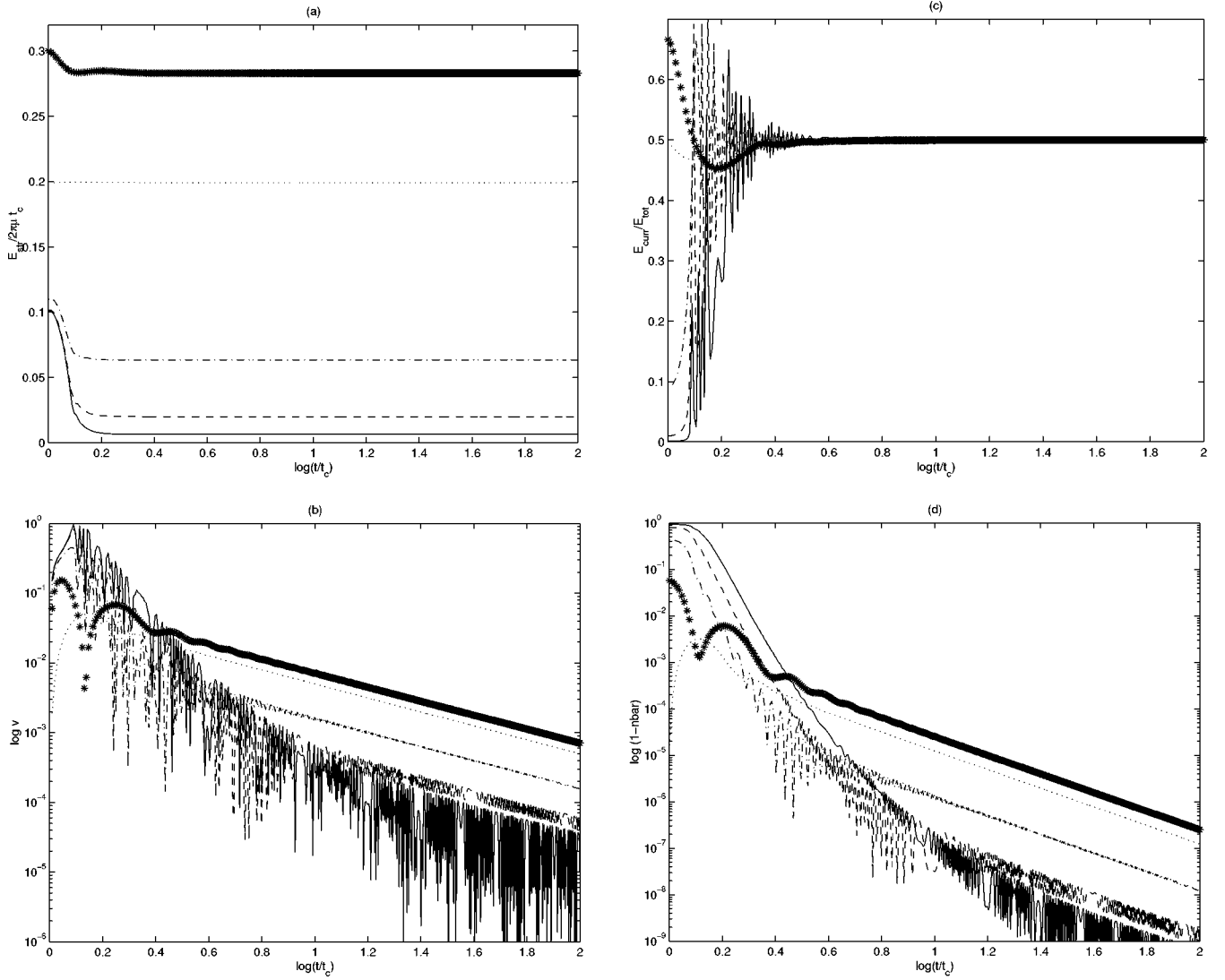


FIG. 5. The evolution of chiral circular GUT-scale string loops formed at $t = t_c$. All loops have an initial string energy $E_{string}/2\pi\mu t_c = 0.1$, but different initial ratios of energies in the current and the string—the cases 10^{-3} , 10^{-2} , 10^{-1} , 1.0 and 2.0 are respectively shown in solid, dashed, dash-dotted, dotted and starred lines. Plots show the total energy E_{total} relative to t_c (a), the (base-10) logarithm of the microscopic velocity (b), the fraction of the loop’s energy in the current (c) and the (base-10) logarithm of the parameter $1 - \bar{n}$ (d).

value of \bar{n} once the loop is “free”—that is, much smaller than the damping length defined in Eq. (2.22).

On the other hand, radiative backreaction also tends to damp these energy oscillations, and consequently increase \bar{n} . Note that this has been shown to have the approximate form $\dot{E} = \Gamma_{em} J^2$, and since $\Gamma_{em} m \sim 100$, the time scale for this process is expected to be relatively short.

Note that when loops become smaller than the damping length scale l_d and reach the “free” regime the following averages over a period hold (note that \bar{n} becomes a constant in this limit—hence its usefulness):

$$\langle \dot{r}^2 \rangle = \frac{1}{2} (1 - \bar{n}^2), \quad (5.10)$$

$$\left\langle \frac{E_{string}}{E_{total}} \right\rangle = 1 - \frac{1}{2} \bar{n}, \quad (5.11)$$

$$\left\langle \frac{E_{string}^2}{E_{total}^2} \right\rangle = 1 - \frac{3}{4} \bar{n}; \quad (5.12)$$

the variance of the fraction of the energy in string is therefore

$$\Delta \frac{E_{string}}{E_{total}} = \frac{1}{4} \bar{n} (1 - \bar{n}). \quad (5.13)$$

In Fig. 4 we show chiral loops with the same initial conditions as Fig. 3, but starting to evolve at the epoch t_* when friction becomes negligible [7]. The differences are self-evident. Now, after a first period of growth of the total radius due to expansion, there is no mechanism forcing the loops to return this extra energy back to the medium when they fall inside the horizon. Consequently there is also no velocity damping (all loops will have microscopic velocities larger than 0.5) and the energy oscillations between the

string and the current always have a large amplitude—so that \bar{n} will never stabilize close to unity when the loops fall inside the horizon.

Note that a loop with a very high initial current will again “overshoots,” but unlike in the case with friction here it can actually end up oscillating faster than another one in the “current branch” but with a smaller current. This is because now there is no friction force that can damp this velocity overshoot.

It can therefore be seen that vortons can only form during the friction-dominated epoch (as we expected), and also that the earlier a loop is formed, the larger will be the region of the space of initial conditions that will originate them—because as we said the effect of friction is to increase \bar{n} . Therefore, for cosmic strings formed at the GUT phase transition, the most favorable case for vorton formation is having the strings becoming superconducting at the GUT scale as well. We will use this assumption in the remainder of the paper.

Finally, in Fig. 5 we plot the more realistic case of the evolution of GUT-scale loops having an initial string radius 10 times smaller than the horizon, and different initial ratios of energies in the current and in the string—ranging from 10^{-3} to 2.

Now the total radius only suffers a small decrease, except in the case where one starts with $\bar{n} \sim 1$, in which case the velocity is so small that friction does not significantly affect the loop. Note that as \bar{n} approaches unity we have $v \propto t^{-1}$ as we predicted, although for loops in the string branch there is an initial transient where $v \propto t^{-4}$. Nevertheless, in the string branch loops do reach fairly high velocities during their first few oscillations, so that once more the issue of whether or not these become vortons is not entirely straightforward.

Also note that for loops of this size the amplitude of the energy oscillations between the string and the current is negligibly small, except for the short transient period (typically lasting less than one Hubble time) for loops in the “string branch” with fairly small currents. Clearly the relation between the initial conditions and the values of \bar{n} and v needs to be looked at in more detail, and we shall do that in the next section.

VI. CRITERIA FOR VORTON FORMATION

In the previous section we saw that the evolution of chiral superconducting cosmic string loops depends sensitively on the conditions at formation. In particular, one would need to know in which cases one ends up with a vorton.

Clearly, since we are not including radiative mechanisms at this stage, our criterion should be that loops whose velocity is always small (in a sense that will need to be made more precise) will become vortons, while those that are relativistic at some stage will suffer significant charge losses, so that their fate cannot be clearly asserted until a rigorous quantum-mechanical treatment of these processes is available.

Thus we will explore in more detail the phase space of possible initial conditions in order to determine relevant properties of these loops. Figure 6 shows the maximum microscopic velocity $v_{max}(l_i, t_i, \bar{n}_i)$ reached by GUT loops formed at $t = t_c, 10t_c, 100t_c$ and $t_* \sim 855t_c$, respectively; it is

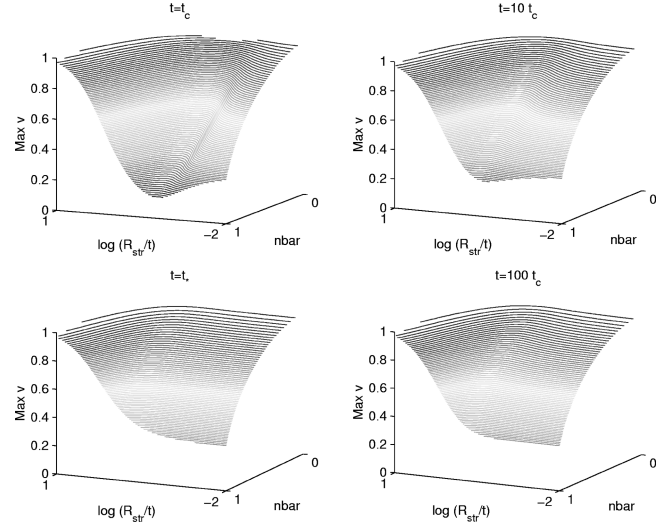


FIG. 6. The maximum microscopic velocity reached by circular GUT-scale chiral superconducting string loops formed at a time $t_f = t_c \sim 10^{-39}$ s (top left) and $t_f = 10t_c, 100t_c, 855t_c$ (clockwise), the latter being t_* . The x axis corresponds to the initial value of the parameter \bar{n} , going from zero (the Goto-Nambu case) to unity; in the y axis the base-10 logarithm of the string radius relative to the horizon size goes from -2 to 1 . Note that in the first graph the friction length scale corresponds to $\log l_f/t \sim -1.5$, while in the last one $\log l_f/t = 0$.

assumed that all such loops start their evolution with a negligibly small velocity—a reasonable assumption, since the network dynamics is friction dominated until t_* . In each case the horizontal axes correspond to the initial value of \bar{n} and to the base-10 logarithm of the initial string radius relative to the horizon; recall that we only consider loops having initially most of their energy in the string (in other words, loops in the string branch). Note that the friction length scale corresponds to about -1.5 in the vertical axis on the first plot and to 0 on the last (where it is equal to the horizon, by definition).

It can be seen that any loop initially larger than the horizon will inevitably become relativistic. This is essentially because expansion will (temporarily, at least) decrease the fraction of the loop’s energy in the current (and hence \bar{n}). On the other hand, loops smaller than the friction length (and the horizon) have essentially no mechanism that can change \bar{n} (neglecting radiation), and so we will need fairly high initial currents in order to get non-relativistic velocities.

Finally, for the case of loops being produced with sizes between the friction length scale and the horizon, which is of course the cosmologically relevant case during the friction-dominated epoch [7], friction will force the loop to shrink (thereby increasing \bar{n}), while the effect of the cosmological expansion will be small, and so in order to have non-relativistic velocities we are allowed to have smaller initial values of \bar{n} than in the previous case.

From the analysis of Figs. 3–6 one can see that we need fairly high values of \bar{n} when the loops reach the “free” regime in order to have reasonable chances of producing GUT vortons in the “string branch.” Now, according to Ref.

[4], the energy of a superconducting loop configuration with radius R is approximately

$$E = 2\pi\mu R + 2\pi\Sigma \frac{W^2}{R} = E_{string} + E_{current}, \quad (6.1)$$

where W is the winding number and $2\pi\Sigma W \sim N_L^{1/2}$ is the net particle number. The parameter Σ is the result of an integral over the string cross section; it is a variable in general, but a constant in the chiral case, and expected to be of the order of the inverse of a coupling constant, $\Sigma \gtrsim 20$; we will in fact take $\Sigma = 20$ unless otherwise stated. This is minimized for a radius

$$\frac{R_v}{W} = \left(\frac{\Sigma}{\mu}\right)^{1/2}; \quad (6.2)$$

this corresponds to a vorton state. As expected, this minimum value is $E_v = 2E_{string}$ and corresponds to $\bar{n} = 1$.

Now, suppose that the energy of a given configuration is a little higher than this minimum. That is, let $E = (1+x)E_v$. Then such a configuration will have a radius

$$\frac{R_{string}}{R_v} = 1+x \pm [(1+x)^2 - 1]^{1/2}; \quad (6.3)$$

we will choose the plus sign since it corresponds to the ‘‘string branch.’’ Then we can use Eq. (5.9) to find the corresponding value of \bar{n} :

$$\bar{n} = 2 \frac{1+x + \sqrt{x(2+x)}}{1 + [1+x + \sqrt{x(2+x)}]^2}. \quad (6.4)$$

These are useful expressions to introduce ‘‘phenomenological’’ criteria for deciding which loop configurations will produce vortons. We note that these should be established on the basis of more detailed numerical studies of the microphysics of the currents; in particular, significant model dependence is of course expected.

As an example, if we take as a necessary condition for vorton formation that the energy of a given configuration be at most 10% higher than E_v , we find that the value of \bar{n} once the loop size becomes smaller than the damping length should obey

$$\bar{n}_{free} \gtrsim \frac{10}{11} \sim 0.91, \quad (6.5)$$

or equivalently that the average fraction of the loop’s energy in the current must be

$$\left\langle \frac{E_{current}}{E_{total}} \right\rangle_T \gtrsim 0.45. \quad (6.6)$$

Another (approximately) equivalent way of stating this is that a loop will not form a vorton state if it exceeds some maximum velocity v_{vor} above which charge and current losses become effective. Note that a fast-moving loop will tend to develop cusps at which such losses should be particu-

larly significant. Hence we require that $v_{max} < v_{vor}$ if a given loop is to form a vorton. Of course v_{vor} depends on x ; for $x = 0.1$, we have

$$v_{vor} \sim 0.29. \quad (6.7)$$

Such a velocity limit is physically plausible, but a rigorous quantum mechanical treatment will be required to obtain more precise values. Note that the size of this vorton-forming region of parameter space is maximal at t_c and decreases with time, vanishing not later than t_* .

If we choose less stringent criteria, say $x = 0.5$ or even $x = 1.0$, our bounds will respectively be

$$\bar{n}_{free} \gtrsim \frac{2}{3}, \quad v_{vor} \sim 0.53, \quad (6.8)$$

$$\bar{n}_{free} \gtrsim \frac{1}{2}, \quad v_{vor} \sim 0.61; \quad (6.9)$$

we will comment on the importance of the precise choice of x in Sec. IX.

Clearly, this only solves half of the problem—the other half is determining what exactly are the initial conditions at the formation of these loops, and in particular what are their currents. In other words, we need to know where in Fig. 6 do the loops form. This is a non-trivial problem, but we will discuss a simplified ‘‘toy model’’ for current evolution in the following section.

VII. EVOLUTION OF THE CURRENTS

Because of the strings’ statistical nature, analytic evolution methods must be ‘‘thermodynamic;’’ that is, one must describe the network by a small number of macroscopic (or ‘‘averaged’’) quantities whose evolution equations are derived from the microscopic string equations of motion. The first such model providing a quantitative picture of the complete evolution of a string network (and the corresponding loop population) has been recently developed by the present authors [7], and we briefly summarize it here.

We start by defining our averaged quantities, the energy of a piece of string,

$$E = \mu a(\tau) \int \epsilon d\sigma \quad (7.1)$$

(ϵ being the coordinate energy per unit σ), and the string rms velocity, defined by

$$v^2 = \frac{\int \dot{\mathbf{x}}^2 \epsilon d\sigma}{\int \epsilon d\sigma}. \quad (7.2)$$

Distinguishing between long (or ‘‘infinite’’) strings and loops, and knowing that the former should be Brownian, we can define the long-string correlation length as $\rho_\infty \equiv \mu/L^2$ (see [7] for an extensive discussion of these quantities and others to be introduced below). A phenomenological term must then be included for the interchange of energy between long strings and loops. A ‘‘loop chopping efficiency’’ pa-

parameter, expected to be slightly smaller than unity, is introduced to characterize loop production:

$$\left(\frac{d\rho_\infty}{dt}\right)_{\text{to loops}} = \tilde{c}v_\infty \frac{\rho_\infty}{L}. \quad (7.3)$$

One can then derive the evolution equation for the correlation length L [7], which has the form

$$2\frac{dL}{dt} = 2HL(1+v_\infty^2) + v_\infty^2 \frac{L}{l_f} + \tilde{c}v_\infty; \quad (7.4)$$

we point out again that the ‘‘friction length scale’’ l_f will in general be that due to Everett scattering.

One can also derive an evolution equation for the long string velocity with only a little more than Newton’s second law:

$$\frac{dv}{dt} = (1-v^2) \left[\frac{k}{L} - v \left(2H + \frac{1}{l_f} \right) \right]; \quad (7.5)$$

here k is another phenomenological parameter that is equal to unity during the friction-dominated epoch and of order unity later [7].

Finally, a careful analysis of the loop production mechanism leads to an expression for the energy density in loops. The idea is that at a given time one looks back at all the loops that have formed (and still have not decayed), finds their present lengths and then adds them together. Distinguishing between ‘‘dynamical’’ and ‘‘primordial’’ (that is, Vachaspati-Vilenkin) loops, we have

$$\begin{aligned} \rho_0(t) = & \int_{t_c}^t n_{\text{dyn}}(t,t') l(t,t') dt' \\ & + \int_{L_c}^{L_{\text{cut}}} n_{\text{pri}}(l',t) l_{\text{pri}}(l',t) dl'. \end{aligned} \quad (7.6)$$

Above $l(t,t')$ is the length at time t of a loop produced at time t' (this will vanish if the loop has decayed), while $n_{\text{dyn}}(t,t')a^3(t) = n_{\text{loop}}(t')a^3(t')$, where

$$n_{\text{loop}}(t) = g\mu\tilde{c} \frac{v_\infty}{\alpha L^4} \quad (7.7)$$

is the number of loops produced per unit time per unit volume. The factor $g \sim 1/\sqrt{2}$ accounts for the fact that not all of the energy lost by the long-string network ends up in the loops—part of it is lost by velocity redshift. We are assuming that loops produced at time t have an initial length $l(t) = \alpha(t)L(t)$ —in other words, that loop production is ‘‘monochromatic’’ (see [7] for a discussion of this point). Similarly, for the Vachaspati-Vilenkin loops $l_{\text{pri}}(l',t)$ is the length at time t of a loop formed with length l' , while $n_{\text{pri}}(l',t)a^3(t) = n_{\text{loop}}(l')a^3(t_c)$, where $n_{\text{loop}}(l')$ is the well-known Vachaspati-Vilenkin loop distribution.

The above quantities are sufficient to quantitatively describe the large-scale characteristics of a cosmic string network. We will describe the evolution of the currents by a recently introduced toy model [11], which we now discuss in more detail.

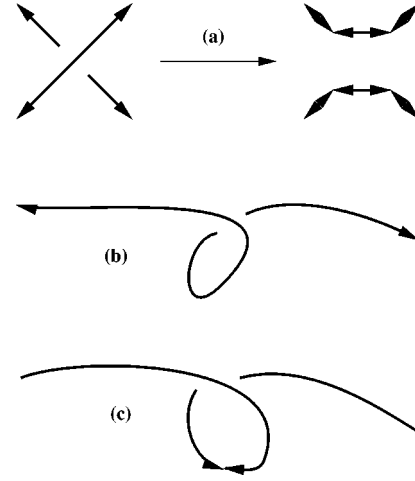


FIG. 7. Some relevant inter-commuting configurations. The arrows mark the limits of regions with correlated currents. Plot (a) shows a typical inter-commuting creating four new current regions, while (b),(c) show that on scales smaller than the current correlation length loop production may (c) or may not (b) remove current regions from the long-string network.

Our analysis will be based on the assumption that there is a ‘‘superconducting correlation length,’’ denoted ξ , which measures the scale over which one has coherent current and charge densities on the strings. Associated with this we can define N to be the number of uncorrelated current regions (in the long-string network) in a co-moving volume $V = a^3 L_0^3$ as follows:

$$N \equiv \frac{L_\infty}{\xi} = \frac{V}{\xi L^2}, \quad (7.8)$$

where L_∞ is the total long string length in the co-moving volume.

Now, ξ and N will obviously change in the course of the evolution of the string network, and we can immediately identify four possible sources of change—expansion, inter-commuting, loop production and internal dynamics on the string worldsheet. We now consider each one of them. First, we expect that in a co-moving volume the number of uncorrelated regions will not be affected by expansion, and so

$$\left(\frac{dN}{dt}\right)_{\text{expansion}} = 0. \quad (7.9)$$

Now consider the effect of inter-commutings (whether or not a loop is produced). Laguna and Matzner [17] have numerically shown that whenever two current-carrying strings cross, they inter-commute and a region of intermediate current is created. This means that inter-commutings will in general create four new regions [see Fig. 7(a)]. Since according to our analytic evolution model the inter-commuting rate is

$$\left(\frac{dn}{dt}\right)_{\text{intercommuting}} = \frac{1}{2} \frac{v_\infty}{\alpha} \frac{V}{L^4}, \quad (7.10)$$

we immediately obtain the following effect on N :

$$\left(\frac{dN}{dt}\right)_{intercommuting} = 2\frac{v_\infty}{\alpha} \frac{V}{L^4}; \quad (7.11)$$

again this assumes that loops have a size $l(t) = \alpha(t)L(t)$ at formation, and that once the long-string network reaches the linear scaling regime we have $\alpha(t) = \alpha_{sc} = \text{const}$ (see [7]).

However, an important correction is necessary to account for the fact that when regions with size of order ξ or smaller self-intersect it is possible [see Figs. 7(b),7(c)] that no new regions are produced. Thus we must multiply Eq. (7.11) by a correction factor

$$F_1\left(\frac{l}{\xi}\right) = 1, \quad \frac{l}{\xi} > 1 \quad (7.12)$$

$$F_1\left(\frac{l}{\xi}\right) = \alpha \left[1 - 2\tilde{c} \left(1 - \frac{l}{\xi} \right) \right] + (1 - \alpha) \frac{l}{\xi}, \quad \frac{l}{\xi} \leq 1. \quad (7.13)$$

The slightly complicated behavior of F_1 is nevertheless easy to understand. The point is that numerical simulations show that there are two types of inter-commutings. First, ‘‘large-scale’’ ones always occur at a scale L ; a fraction α of the inter-commutings should be of this type. If this happens between two long-strings (that is, no loop is produced), we always expect to create new regions, since there is no reason for currents in different ‘‘infinite’’ strings to be correlated. On the other hand, if what we have is a long string self-intersecting to produce a loop of size smaller than ξ (a fraction $2\tilde{c}$ of these inter-commutings should produce loops), then we might not form new regions—for each length, the fraction of these self-intersections that produce new regions is essentially given by the ratio of the size of the region and the superconducting correlation length. The remainder of the inter-commutings are associated with the presence of small-scale structure on the strings, and occur by repeated self-intersections of a given string, and so the l/ξ cutoff always applies. Notice that the second term vanishes if $\alpha = 1$ (as it should) but it rapidly becomes dominant as α starts deviating from unity. Also note that the overall inter-commuting effect is approximately α independent (more on this below).

Of course, when the inter-commuting does produce a loop, the regions in the corresponding segment are removed from the network, together with one of the newly created ‘‘intermediate’’ regions, and we similarly have

$$\left(\frac{dN}{dt}\right)_{loops} = -\left(\frac{l}{\xi} + 2F_2\right) \tilde{c} \frac{v_\infty}{\alpha} \frac{V}{L^4}, \quad (7.14)$$

where the analogous correction factor F_2 is of the form

$$F_2\left(\frac{l}{\xi}\right) = 1, \quad \frac{l}{\xi} > 1 \quad (7.15)$$

$$F_2\left(\frac{l}{\xi}\right) = \frac{l}{\xi}, \quad \frac{l}{\xi} \leq 1. \quad (7.16)$$

Note that string length is always removed from the long string network when loops form, regardless of whether or not current regions are. This is in fact the main effect of loop production, as can be seen by noting that Eq. (7.14) is ap-

proximately independent of the parameter characterizing the loop size, α . In the friction-dominated regime, α is of order unity, and when it becomes much smaller (in the free regime) the α dependences in the numerator and in the denominator cancel out. One can readily see that this is physically plausible: when $\alpha \sim 1$ (in the friction-dominated epoch) few loops are produced, but each one of them removes a significant number of regions; on the other hand, when α is small, many more loops are produced, but only a few of them will remove regions.

Finally, there is the dynamic term. When regions with opposite currents inter-commute, new charged regions are created, setting up alternate currents. One expects electromagnetic processes to make these currents die down, so that the charged region will eventually equilibrate with its neighbors. The simulations of Laguna and Matzner [17] provide qualitative support for this intuitive picture. Clearly, this indicates that some kind of ‘‘equilibration’’ process is effectively acting between neighboring current regions, which will counteract the creation of new regions by inter-commuting. While it is beyond our means to derive an ‘‘equilibration term’’ from first principles we will, as a first approximation, introduce a phenomenological term. We will model this current decay by assuming that after each Hubble time, a fraction f of the N regions existing at its start will have equilibrated with one of its neighbors:

$$\left(\frac{dN}{dt}\right)_{dynamics} = -fHN; \quad (7.17)$$

note that new regions are obviously created by inter-commuting during the Hubble time in question, so that f can be larger than unity. Alternatively we can say that for a given f , the number of regions in a given volume at a time t will have disappeared due to equilibration at a time $t + (fH)^{-1}$. We therefore obtain the following evolution equation for N :

$$\frac{dN}{dt} = G\left(\frac{l}{\xi}\right) \frac{v_\infty}{\alpha} \frac{V}{L^4} - fHN, \quad (7.18)$$

where we have re-defined the correction factor

$$G\left(\frac{l}{\xi}\right) = 2 - \tilde{c} \left(\frac{l}{\xi} + 2 \right), \quad \frac{l}{\xi} > 1 \quad (7.19)$$

$$G\left(\frac{l}{\xi}\right) = 2(1 - 2\tilde{c})\alpha + (2 - 3\tilde{c} - 2\alpha + 4\alpha\tilde{c}) \frac{l}{\xi}, \quad \frac{l}{\xi} \leq 1. \quad (7.20)$$

Note that when $l \gg \xi$ the net effect of inter-commuting and loop production is to remove uncorrelated regions (because each loop formed removes a large number of them); otherwise, the net effect is to create new regions.

However, for what follows it is convenient to re-write it in two alternative forms. First, we can define N_L to be the number of uncorrelated current regions per long-string correlation length:

$$N_L \equiv \frac{L}{\xi} = N \frac{L}{L_\infty}; \quad (7.21)$$

this is useful because, as was first pointed out by Davis and Shellard [4], we expect the net charge of a superconducting loop to be given by

$$Q \sim eN_L^{1/2}. \quad (7.22)$$

In terms of N_L , Eq. (7.18) has the form

$$\frac{dN_L}{dt} = (3v_\infty^2 - f)HN_L + \frac{3}{2} \frac{v_\infty^2}{l_f} N_L + \left(\frac{1}{\alpha} G(\alpha N_L) + \frac{3}{2} \tilde{c} N_L \right) \frac{v_\infty}{L}; \quad (7.23)$$

note that to obtain this one needs to substitute the evolution equation for the long-string correlation length L , Eq. (7.4), and that one can equivalently define G as

$$G(\alpha N_L) = 2 - \tilde{c}(\alpha N_L + 2), \quad \alpha N_L > 1, \quad (7.24)$$

$$G(\alpha N_L) = 2(1 - 2\tilde{c})\alpha + (2 - 3\tilde{c} - 2\alpha + 4\alpha\tilde{c})\alpha N_L, \quad \alpha N_L \leq 1. \quad (7.25)$$

Yet another useful form follows from defining N_H to be the number of uncorrelated current regions in one Hubble volume,

$$N_H \equiv \frac{L_H}{\xi} = N_L \frac{d_H^3}{L^3}; \quad (7.26)$$

in this case we have

$$\frac{dN_H}{dt} = (3 - f)HN_H + G(\alpha N_L) \frac{v_\infty}{\alpha} \frac{d_H^3}{L^4}. \quad (7.27)$$

VIII. IMPORTANCE OF EQUILIBRATION

Now the question is, of course, what is f ? From a more intuitive point of view, an equivalent question is the following: given a particular piece of string with a given current, is it more likely to disappear from the network by this equilibration mechanism or by being incorporated in a loop? Even though a precise answer can probably only be given by means of a numerical simulation, some very simple physical arguments can be used to restrict it. We should point out, however, that many of the results of the following sections do not depend crucially on the value of f .

First, correlations cannot obviously be established faster than the speed of light (that is, we must have $\xi \leq t$), so that we should impose that

$$\left(\frac{dN_H}{dt} \right)_{N_H=L_H/t} \geq 0; \quad (8.1)$$

this leads to an upper bound on f , which we can write, defining $L = \gamma t$, as

$$f_{max}(\tilde{c}, \gamma, v_\infty) = 3 + 4(1 - 2\tilde{c}) \frac{v_\infty}{\gamma^2}. \quad (8.2)$$

(In this section we will concentrate on the bounds on f in the radiation epoch—analogous results can be obtained for the mat-

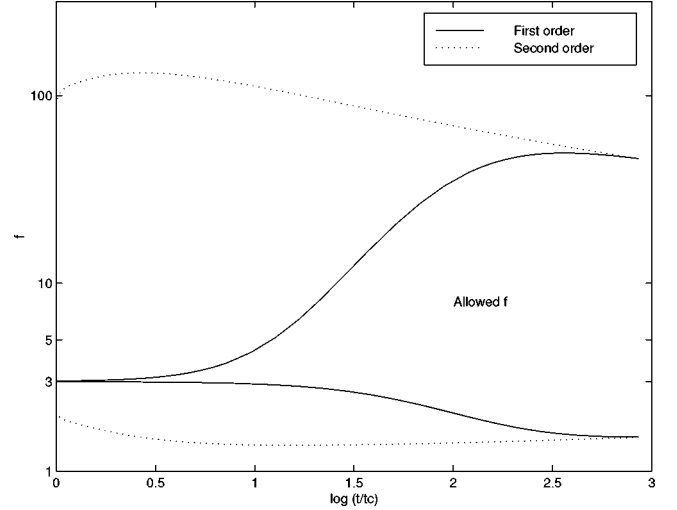


FIG. 8. The evolution of f_{min} (lower pair of curves) and f_{max} (upper pair of curves) for first order (solid lines) and second order (dotted lines) string-forming phase transitions. Time is in orders of magnitude from the epoch of string formation.

ter epoch.) We explicitly write the dependences of f_{max} to emphasize that this is the maximum value of f which satisfies Eq. (8.1) for a given set of properties of the cosmic string network.

On the other hand, if an equilibration mechanism such as that modelled by Eq. (7.17) exists [17], it is reasonable to assume that it will prevent N_H from growing without limit—possibly through a backreaction mechanism as in the case of gravitational radiation for wiggly Goto-Nambu strings—and eventually it will make it become constant (meaning that ξ is scaling linearly). In other words, we can assume that there should be a large N_H^* (which we need not specify) such that

$$\left(\frac{dN_H}{dt} \right)_{N_H^*} \leq 0; \quad (8.3)$$

we can therefore find a lower bound on f which satisfies this,

$$f_{min}(\tilde{c}, \gamma, v_\infty) = 3 - 2\tilde{c} \frac{v_\infty}{\gamma}. \quad (8.4)$$

Again this varies as the network evolves. Note that the crucial point about this construction is that Eq. (7.17) depends linearly on N_H .

Using the quantitative evolution model of the present authors we have plotted f_{max} and f_{min} during the friction-dominated epoch with initial conditions typical of first and second order phase transitions, in Fig. 8. These plots are fairly easy to interpret. Perhaps the most surprising result is the large values of f_{max} allowed when the long-string correlation length is well below the horizon. This is because in this case the loops chopped off by the network are small, so that each one of them removes relatively few current regions—one could therefore have an extremely efficient equilibration mechanism and still obey the constraint (8.1). Hence we can see from Fig. 8 that if our toy model, and in particular the *Ansatz* (7.17), is valid, the constraints on f are much stronger for a first-order phase transition. One can also

see that $f=3$ is the only value that is acceptable at all times, regardless of the initial condition. However, it is at present unclear if there is something ‘‘special’’ about this value. A numerical simulation is presumably the only way to clarify this issue.

Note that any value $f_{min} < f < f_{max}$, once the network reaches the linear scaling regime

$$1.88 \sim 3 - \frac{2\tilde{c}}{k+\tilde{c}} < f < 3 + \frac{4(1-2\tilde{c})}{k^{1/2}(k+\tilde{c})^{3/2}} \sim 22.4, \quad (8.5)$$

leads to a constant value of N_L and that this corresponds to ξ scaling as the long-string correlation length L . Different values of f lead to different scaling values of N_L (with larger f 's corresponding to smaller N_L 's as expected) at least in some region of the space of initial conditions, but for any $f \neq 3$ one can think of some set of physically viable initial conditions for which either causality would be violated at some stage of the evolution or the number of uncorrelated regions would grow without bound. The scaling value of N_L can be written in terms of the properties of the string network as

$$\alpha_{sc} N_L = \frac{4(1-\tilde{c})}{(k+\tilde{c})f - \tilde{c} - 3k}; \quad (8.6)$$

one can see that in this regime the f dependence is rather weak, unless f is just above f_{min} .

We emphasize that while the f_{max} bound is unavoidable (being a consequence of causality), f_{min} is less robust and could well be disproved by a detailed numerical study. Therefore, in what follows we will discuss two cases, $f=0$ and $f=3$, which should represent the scenarios of ineffective (or non-existent) and effective equilibration.

For a given f , we can now solve Eq. (7.23) numerically, coupled with the evolution equations for the long-string correlation length and average velocity (see [7]). This therefore allows us to know the size of the loops formed by the network at each time and [through Eq. (7.22)] the initial current they will carry. One is then in a position of applying the criteria established in Sec. VI in order to decide whether or not each loop will form a vorton.

We should also say at this stage that once the network leaves the friction-dominated regime and strings become relativistic other mechanisms (notably radiation) can cause charge losses in the long strings (as well as in loops). Hence our toy model can at best provide order-of-magnitude estimates in this regime. On the other hand, we expect it to be quite accurate (pending a more detailed numerical study) in the friction-dominated epoch—which is of course relevant for vorton formation.

IX. GUT-SCALE ANALYSIS

In Figs. 9 and 10 we plot the result of the numerical integration of Eq. (7.23), for initial conditions representative of string-forming and superconducting phase transitions of first and second order, for the cases $f=0$ and $f=3$. We are assuming that these occur at around the same (GUT) energy scale since, as we have shown in Sec. VI, this is most favorable situation for vorton formation. It was also assumed that

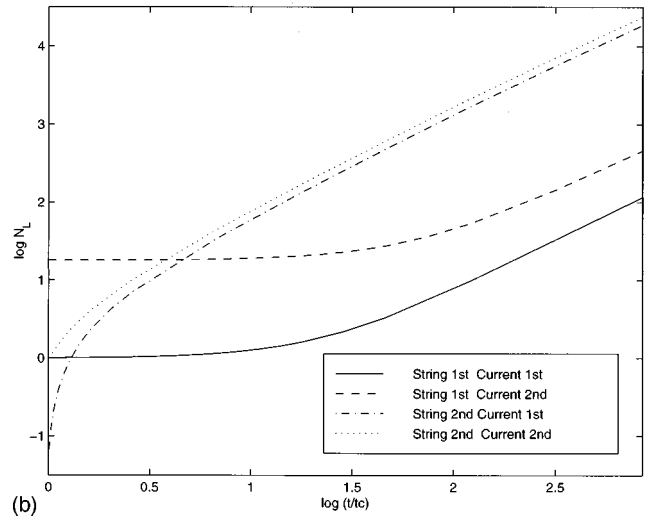
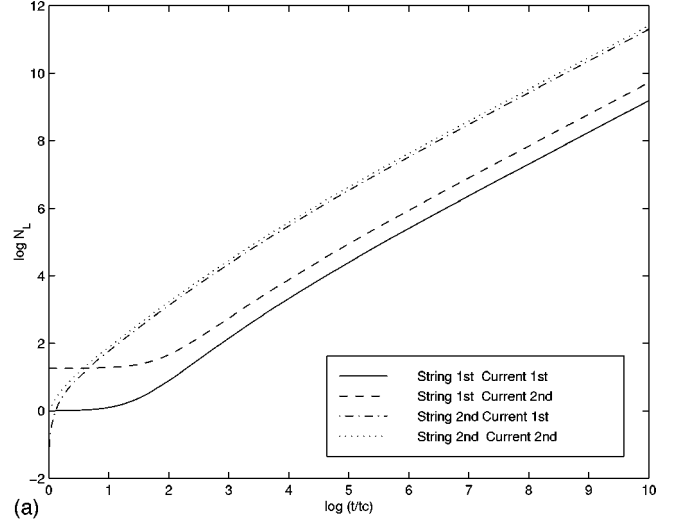


FIG. 9. The evolution of the number of uncorrelated current regions per long-string correlation length, N_L , for the case $f=0$ (the bottom plot is a friction-dominated epoch closeup of the top one) assuming that the orders of the string-forming and superconducting phase transitions are respectively: 1st and 1st (solid lines), 1st and 2nd (dashed lines), 2nd and 1st (dash-dotted lines) and 2nd and 2nd (dotted lines). Time is in orders of magnitude from the epoch of string formation.

the value of α in the linear scaling regime is $\alpha_{sc} \sim 10^{-3}$ (see Ref. [7]).

The differences between the two cases are considerable. First, if there is no equilibration mechanism ($f=0$; see Fig. 9), the number of uncorrelated regions per long-string correlation length, N_L , never decreases. In this case there are simple scaling laws for N_L and ξ . One finds that ξ is conformally stretched during the stretching regime (just like the long-string correlation length, $L \propto t^{1/2}$), and so N_L is approximately constant. However, as inter-commutings start creating new regions N_L begins to increase, and it grows as $t^{3/2}$ during the Kibble regime (where $L \propto t^{5/4}$, and so $\xi \propto t^{-1/4}$). Finally, once the network reaches the linear scaling regime, $L \propto t$, the number of uncorrelated current regions grows as $N_L \propto t$, which corresponds to $\xi \propto \text{const}$. As expected, in this case the network keeps a ‘‘memory’’ of its initial conditions.

On the other hand, if there is an efficient enough equili-

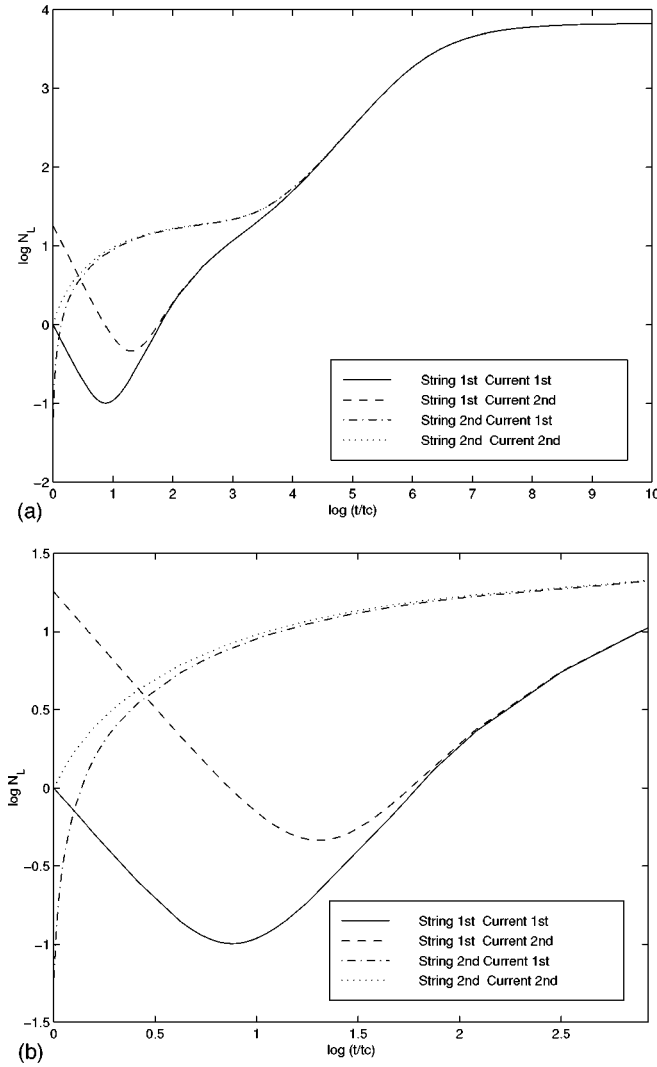


FIG. 10. The evolution of the number of uncorrelated current regions per long-string correlation length, N_L , for the case $f=3$ (the bottom plot is a friction-dominated epoch closeup of the top one) assuming that the orders of the string-forming and superconducting phase transitions are respectively: 1st and 1st (solid lines), 1st and 2nd (dashed lines), 2nd and 1st (dash-dotted lines) and 2nd and 2nd (dotted lines). Time is in orders of magnitude from the epoch of string formation.

bration mechanism (see Fig. 10 for the case $f=3$), then N_L decreases while the network is being conformally stretched. In the Kibble regime, the increased number of intercommutings again drives N_L up, and after α has evolved into its linear regime value, ξ itself reaches a scaling value and hence N_L becomes a constant. In the intermediate case of a small but non-zero f , N_L decreases during the stretching regime but grows without limit afterwards, and the precise values of the scaling laws depend on f . Also, the network will preserve a “memory” of the order of the string-forming phase transition, but not of the order of the superconducting one.

This therefore solves the other half of our problem. Knowing the loop size at formation at all times [7] at the typical current that each loop carries at that epoch (from the above toy model) one can then apply some criterion (possibly of the type discussed in Sec. VI) to decide which loops

have a reasonable possibility of becoming vortons.

Our quantitative string evolution model [7] allows us to determine the size of the loops formed at each epoch, $l(t) = \alpha(t)L(t)$. On the other hand, according to Eq. (5.9), to find the initial \bar{n} we need to know the ratio of the energies in the string and in the current. Now, the energy of a superconducting loop configuration with a radius R is given by Eq. (6.1), and so after some algebra we find

$$\frac{E_{\text{current}}}{E_{\text{string}}} = \frac{16\pi^3 \mathcal{N}}{45\Sigma} \frac{G\mu N_L}{\alpha^2 \gamma^2 x^2}, \quad (9.1)$$

where $L = \gamma t$, $t = xt_c$ and \mathcal{N} is the number of effectively massless degrees of freedom. Note that the minimum value of γ is of the order of $(G\mu)^{1/2}$ (but slightly larger—see [7]), and so the crucial factor in this equation, and hence for vorton formation, is how much N_L can grow. This alone tells us that the higher the energy scale at which the string network forms, the less likely it is to produce vortons, since it will be friction dominated (and hence non-relativistic) for a shorter period of time. In order to make vortons, loops should be formed with a high enough N_L to allow them to remain non-relativistic thereafter—otherwise, they will eventually become relativistic and hence liable to charge losses. As we already pointed out, making the strings become superconducting sometime after they form does not help—it merely reduces the time available to build up charges and currents.

Contrary to current belief (which is based on rather more qualitative estimates) we do not expect any vortons to be produced by GUT-scale cosmic string networks. In Figs. 11 and 12 we plot the paths of initial conditions in \bar{n} - R space for dynamic and Vachaspati-Vilenkin loops [18] formed during the friction-dominated epoch in the cases $f=0$ and $f=3$. For the “dynamic” loops, we only plot loops formed until $100 t_c$ (notice that \bar{n} decreases after this epoch). We consider initial conditions for the string network that are characteristic of first- and second-order string-forming and superconducting phase transitions. Note that the difference in the initial \bar{n} 's between the two cases is smaller than the difference between the corresponding N_L 's; this is because \bar{n} is approximately proportional to $N_L^{1/2}$.

One can see that, even if we choose the less stringent of our three suggested criteria, calling a vorton any loop configuration with an energy up to twice the minimum value (that is, $x=1$), we still get no GUT vortons. In fact, one would need to choose a limiting velocity $v_{\text{vor}} \sim 0.7$ for GUT vorton production to occur in this model—and even so, only in the case when equilibration is efficient and the string-forming phase transition is of second order. However, we should emphasize that the issues of the precise vorton formation criterion, as well as that of the value of the “equilibration parameter” f , can only be settled by means of more detailed numerical studies of the microphysics of these loop configurations.

This is an appropriate point at which to add a cautionary note about the quantum-mechanical stability of vortons. This is a rather involved and model-dependent question which has

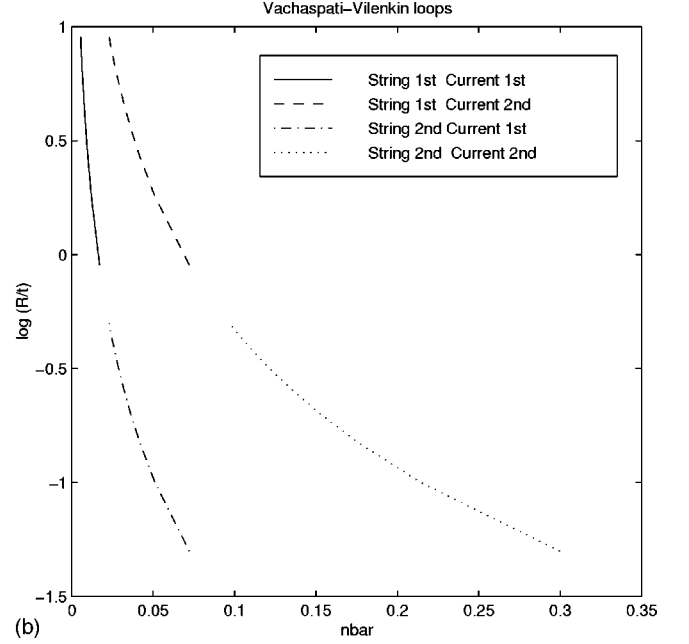
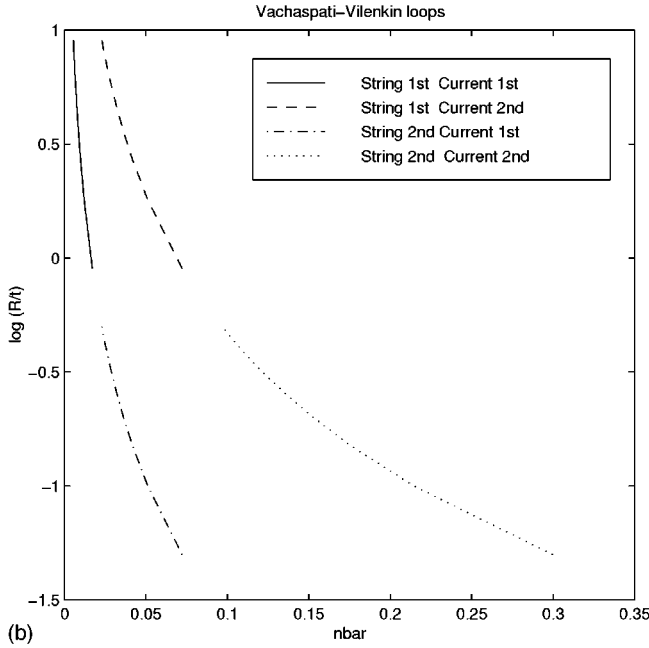
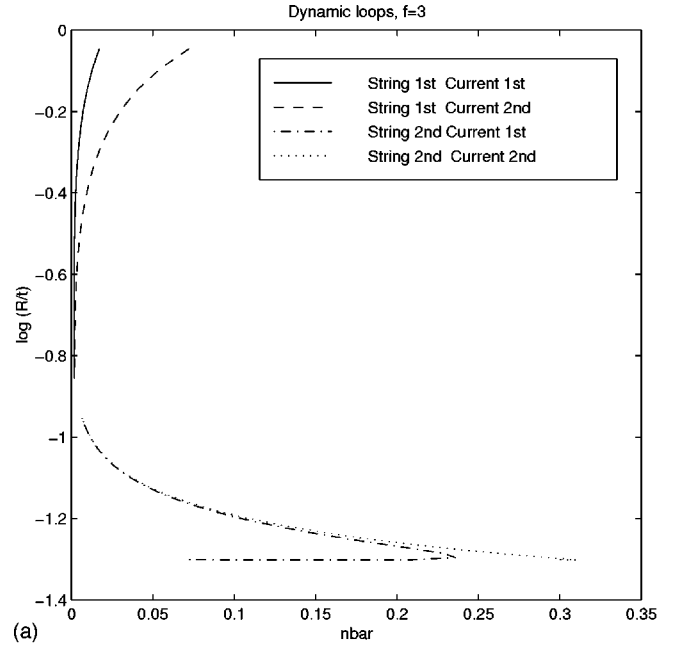
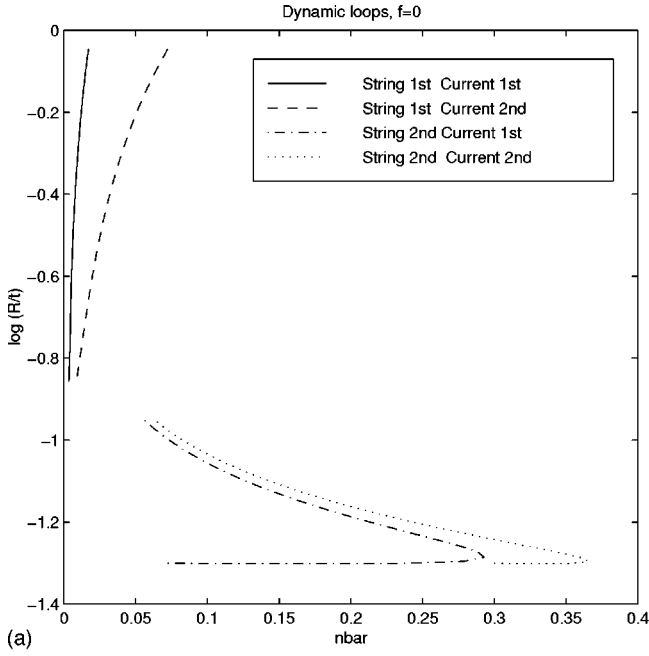


FIG. 11. The initial conditions for loop formation in \bar{n} - R space, for the case $f=0$, assuming that the orders of the string-forming and superconducting phase transitions are, respectively, 1st and 1st (solid lines), 1st and 2nd (dashed lines), 2nd and 1st (dash-dotted lines) and 2nd and 2nd (dotted lines). The top plot corresponds to dynamic loops formed between t_c and $100t_c$ (in the first two curves loops formed at t_c are at large R ; in the latter two they are at small R). The bottom corresponds to “primordial” Vachaspati-Vilenkin loops formed at t_c and having lengths between L_c and $10L_c$.

been briefly discussed in Ref. [4]. The vorton gains additional stability because its charge carriers must tunnel off the string by taking both charge and angular momentum; the larger a vorton is, the more stable it is. With electromagnetic fields present, pair creation provides an alternative decay mechanism, but for a chiral vorton with null fields ($E^2 = B^2$) near the string, this mechanism is strongly suppressed.

FIG. 12. The initial conditions for loop formation in \bar{n} - R space, for the case $f=3$, assuming that the orders of the string-forming and superconducting phase transitions are, respectively, 1st and 1st (solid lines), 1st and 2nd (dashed lines), 2nd and 1st (dash-dotted lines) and 2nd and 2nd (dotted lines). The top plot corresponds to dynamic loops formed between t_c and $100t_c$ (in the first two curves loops formed at t_c are at large R ; in the latter two they are at small R). The bottom corresponds to “primordial” Vachaspati-Vilenkin loops formed at t_c and having lengths between L_c and $10L_c$.

As the chiral state tends to be an attractor for a wide range of initial conditions [3] this again encourages us to believe that vortons should generically be quantum mechanically stable. Nevertheless, one can make special parameter choices for which vorton lifetimes are very brief, notably when the string and current-forming phase transitions are widely separated in energy scale. This subject clearly deserves a more thorough investigation.

X. CALCULATING VORTON DENSITIES

Vorton densities can be calculated using a fairly straightforward modification to the method developed in [7] and summarized above. We now have

$$\rho_v(t) = \int_{t_c}^t W_1(t') n_{dyn}(t, t') l(t, t') dt' \quad (10.1)$$

$$+ \int_{L_c}^{L_{cut}} W_2(l') n_{pri}(l', t) l_{pri}(l', t) dl'. \quad (10.2)$$

The original model for Goto-Nambu strings included an averaged evolution equation for the length l of each loop, which made the above calculation relatively easy. Here, an analogous averaged equation for a superconducting loop is presently unavailable, but the loop size (and velocity) can be determined by evolving the microscopic equation of motion (5.3). The functions $W_1(t')$ and $W_2(l')$ are “window” functions—typically combinations of Heaviside functions—selecting the time interval in the evolution of the network (and the interval in the length of Vachaspati-Vilenkin loops) which will produce vortons, according to the particular criterion that one chooses to impose. Notice that these will depend on a number of parameters, including the initial conditions of the cosmic string network. Also, they should in principle include a factor accounting for the fact that it takes some time for each loop to reach a vorton configuration (that is, even if a given loop will eventually form a vorton, it should not be included in the vorton density until some time after it is “chopped off” from the long-string network). However, note that Fig. 5 seems to indicate that this evolution, if it happens at all, is quite fast—it takes less than one Hubble time.

Note that although in the evolution of the loops the effects of the currents are properly accounted for (with the exception of radiative mechanisms), the evolution of the long string network does not take account of possible effects of the buildup of the currents. Still, we expect the neglect of these effects to be a reasonable assumption. This is because such effects should only become important (if ever) at late times when the network has had time to build up large currents while, as we will shortly see, most of the energy density in vortons is produced fairly soon after the network forms (but a possible exception to this can occur if there are background magnetic fields which can increase the current buildup rate).

Thus calculation of vorton densities is a two-stage process. First, one must study the microphysics of the particular model that one is interested in, in order to derive its microscopic equations of motion and in particular to construct appropriate expressions for the “window functions” $W_1(t')$ and $W_2(l')$ which will determine at which stages of the evolution of the string network one can form vortons. Second, one can use the velocity-dependent one-scale model and the model for the evolution of the currents on the long strings, together with the microscopic loop equations of motion (or an averaged version of them), to determine the vorton density using Eq. (10.2). Typically there will be a single time interval $t_c \leq t_{start} < t < t_{stop} \leq t_*$ at which vortons will form, but it is relatively easy to think of initial conditions for which

vortons form at two different time intervals. Values of t_{start} and t_{stop} in specific models will be discussed in a forthcoming publication [12].

Since, as we pointed out, there is some uncertainty in some crucial parameters of this model, we will limit ourselves in this paper to calculate the vorton density for GUT and electroweak string networks in the “best” (or “worst” according to opinion) possible case where there is no equilibration (that is, $f=0$), the string-forming and superconducting phase transitions are both of second order, and all the loops produce vortons (hence our criterion is simply $\bar{n}_{free} > 0$). Notice that this last condition is unrealistic for GUT networks (where, as we already indicated, we do not expect vortons to form) but is plausible for electroweak networks. Still, we will assume that vortons can only be formed while the network is in the friction-dominated regime. Also, since one presumably needs to have quite efficient radiation mechanisms for all loops to relax into vortons, we will assume that such relaxation is instantaneous—thus $W_2=1$, while W_1 is unity in the friction-dominated epoch and vanishes afterwards.

Figure 13 displays the resulting vorton densities, relative to the background and matter densities. First, we confirm that most of the energy density in vortons is produced soon after the network forms. In the case of GUT strings, we see that vortons would only dominate the energy density of the universe about four orders of magnitude in time after the epoch of network formation, that is soon after friction domination ends (recall that for a GUT network $t_* \sim 850t_c$). Thus, even if all these vortons formed, they would not contradict the standard cosmological scenario provided that they decayed soon after t_* , when the network becomes free. In any case we emphasize that this “worst case” scenario is not realistic for GUT-scale strings, and indeed (as discussed previously) we do not expect GUT-scale vortons to form at all.

On the other hand, electroweak string networks are friction dominated until after the radiation-matter transition, and so the vorton density has been slowly building up relative to that of matter until very recently. We find that this density today would be about 6% of the critical density. On the other hand, a string network formed at $T \sim 10^4$ GeV would provide a maximal vorton density equal to the critical density. This is therefore the strongest possible vorton constraint—it is based on the assumption that all loops form vortons. Naturally, realistic models are not expected to be fully efficient in producing vortons, and furthermore the relevant phase transitions are not necessarily of second order. One can therefore conjecture that the dark matter problem might be solved by a superconducting string network formed at an energy scale of $T \sim 10^5 - 10^6$ GeV. Note that there are a number of supersymmetric models producing such networks (see for example [19]). We will present a more detailed analysis of these issues in a future publication [12].

XI. CONCLUSIONS

In this paper we have presented the first rigorous study of the cosmological evolution of superconducting strings in the limit of chiral currents. We have shown that in this limit the elastic string model of Carter and Peter [10] coincides with the model derived from first principles by Witten [1].

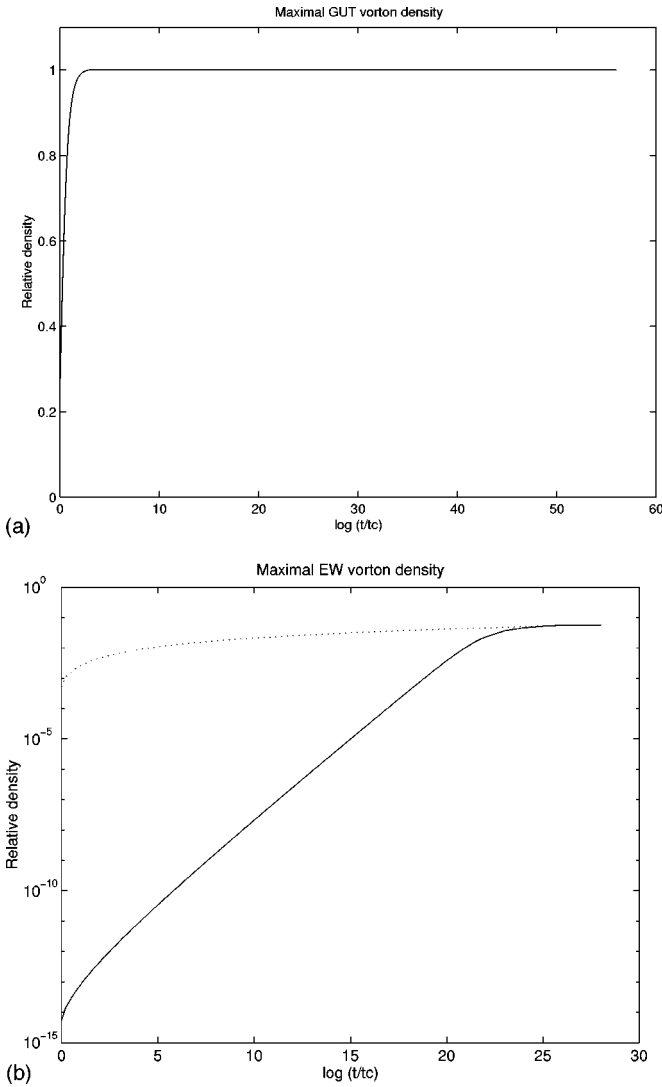


FIG. 13. The maximum possible vorton densities relative to the background (solid lines) and ordinary matter (dotted lines) densities, for GUT- and electroweak-scale string networks. Time is in orders of magnitude from the epoch of string formation; the plots end at the present epoch.

By analyzing physically relevant loop solutions of the microscopic equations of motion for these strings, we have verified that the effect of frictional damping is crucial for vorton formation. We then defined suitable parameters characterizing the evolution of these loops, and in particular whether or not they become vortons. In particular, we have established the usefulness of the “stability parameter” \bar{n} . In general, it is more difficult to form vortons when the string-forming phase transition is of first order. This is because such networks produce, during their evolution in the stretching regime, loops with a size close to that of the horizon; these will therefore be significantly affected by expansion,

which tends to decrease the fraction of the loops’ energy in the current—whereas friction tends to increase it.

After introducing a simple “toy model” for the evolution of currents on the strings [11], we have considered the cases of first- and second-order GUT-scale string-forming and superconducting phase transitions (which is the most favorable GUT case of vorton formation since frictional forces can act longer). We have presented evidence suggesting that GUT-scale string networks might well produce no vortons, and that even if they do, this will not necessarily rule out such models. This is in contradiction with previous, less detailed studies [4,5], and hence calls for a re-examination of a number of cosmological scenarios involving superconducting strings. Notably, these strings could be at the origin of the observed galactic magnetic fields [20].

Finally, we have explicitly calculated the vorton density in two “extreme” cases to illustrate the method that one should follow once the microphysical properties of these networks are known in more detail. For electroweak-scale string networks, we have found that vortons can produce up to about 6% of the critical density of the universe. On the other hand, it is conceivable that superconducting string networks formed at an energy scale $T \sim 10^4 - 10^6$ GeV (depending on details of the model) can solve the dark matter problem.

The detailed analysis presented in this paper for GUT strings can obviously be extended to other energy scales—this will be the subject of a forthcoming publication [12]. Obviously, as we lower the energy scale, the frictional force becomes more and more important and acts for a longer time. Hence the vorton-forming region of parameter space increases, and by the electroweak scale almost all loops chopped off the long-string network will become vortons. We therefore conclude that in addition to the low- $G\mu$ regime (which as we saw includes the electroweak scale) where vortons can be a source of dark matter and to an intermediate- $G\mu$ range in which vortons would be too massive to be compatible with standard cosmology (thereby excluding these models), there is also a high- $G\mu$ regime (of which the GUT scale is part) in which vortons do not form at all and therefore no cosmological constraints based on them can be set. It is then curious (to say the least) that vorton constraints can be used to rule out cosmic string models in a wide range of energy scales $G\mu$, but not those formed around the GUT or the electroweak scales, where cosmic strings can be cosmologically useful.

ACKNOWLEDGMENTS

C.M. is funded by JNICT (Portugal) under “Programa PRAXIS XXI” (Grant No. PRAXIS XXI/BD/3321/94). E.P.S. is funded by PPARC and we both acknowledge the support of PPARC and the EPSRC, in particular the Cambridge Relativity rolling grant (GR/H71550) and a Computational Science Initiative grant (GR/H67652).

[1] E. Witten, Nucl. Phys. **B249**, 557 (1985).

[2] A. Vilenkin and E. P. S. Shellard, *Cosmic Strings and other Topological Defects* (Cambridge University Press, Cambridge, England, 1994).

[3] R. L. Davis and E. P. S. Shellard, Phys. Lett. B **209**, 485 (1988).

[4] R. L. Davis and E. P. S. Shellard, Nucl. Phys. **B249**, 557 (1989).

- [5] R. H. Brandenberger *et al.*, Phys. Rev. D **54**, 6059 (1996).
- [6] B. Carter, in *The Formation and Evolution of Cosmic Strings*, edited by G. W. Gibbons *et al.* (Cambridge University Press, Cambridge, England, 1990); in *Formation and Interactions of Topological Defects*, edited by A. C. Davis and R. H. Brandenberger (Plenum, New York, 1995), and references therein.
- [7] C. J. A. P. Martins and E. P. S. Shellard, Phys. Rev. D **53**, 575 (1996); **54**, 2535 (1996).
- [8] C. J. A. P. Martins and E. P. S. Shellard, Phys. Rev. B **56**, 10 892 (1997).
- [9] C. J. A. P. Martins, Phys. Rev. D **55**, 5208 (1997); P. P. Avelino, R. R. Caldwell, and C. J. A. P. Martins, *ibid.* **56**, 4568 (1997).
- [10] B. Carter and P. Peter, Phys. Rev. D **52**, 1744 (1995).
- [11] C. J. A. P. Martins and E. P. S. Shellard, "Evolution of superconducting string currents," hep-ph/9706533.
- [12] C. J. A. P. Martins and E. P. S. Shellard, "Limits on Cosmic Chiral Vortons," DAMTP Report No. R-98/19.
- [13] A. Vilenkin, Phys. Rev. D **43**, 1060 (1991).
- [14] R. Rohm, Ph.D. thesis, Princeton University, 1985; P. de Sousa Gerbert and R. Jackiw, Commun. Math. Phys. **124**, 229 (1988); M. G. Alford and F. Wilczek, Phys. Rev. Lett. **62**, 1071 (1989).
- [15] B. Carter, Phys. Lett. B **224**, 1961 (1989).
- [16] P. Peter, Phys. Rev. D **45**, 1091 (1992); **46**, 3335 (1992).
- [17] P. Laguna and R. A. Matzner, Phys. Rev. D **41**, 1751 (1990).
- [18] T. Vachaspati and A. Vilenkin, Phys. Rev. D **30**, 2036 (1984).
- [19] A. Riotto, Phys. Lett. B **413**, 22 (1997).
- [20] C. J. A. P. Martins and E. P. S. Shellard, Phys. Rev. D **57**, 5276 (1998).